# DEC1 Regulates Human β Cell Functional Maturation and Circadian Rhythm

Sam Preza[1,2,3], Bliss Zheng[1], Zihan Gao[1,2,3], Mai Liu[1,2,3], Akshaya Biju[1], and Juan R. Alvarez-Dominguez[2,3,4,5*]

[1]Department of Bioengineering, University of Pennsylvania; Philadelphia, PA 19104, USA.

[2]Chronobiology and Sleep Institute, and Institute for Regenerative Medicine, University of Pennsylvania Perelman School of Medicine; Philadelphia, PA 19104, USA.

[3]Institute for Diabetes, Obesity and Metabolism, University of Pennsylvania Perelman School of Medicine; Philadelphia, PA 19104, USA.

[4]Department of Cell and Developmental Biology, University of Pennsylvania Perelman School of Medicine; Philadelphia, PA 19104, USA.

[5]Lead contact

*Correspondence: Juan.Alvarez@pennmedicine.upenn.edu

## SUMMARY

Stem cell-derived islet (SC-islet) organoids offer hope for cell replacement therapy in diabetes, but their immature function remains a challenge. Mature islet function requires the β-cell circadian clock, yet how the clock regulates maturation is unclear. Here, we show that a circadian transcription factor specific to maturing SC-β cells, DEC1, regulates insulin responsiveness to glucose. SC-islet organoids form normally from *DEC1*-ablated human pluripotent stem cells, but their insulin release capacity and glucose threshold fail to increase during *in vitro* culture and upon transplant. This deficit reflects downregulation of maturity-linked effectors of glucose utilization and insulin exocytosis, blunting glycolytic and oxidative metabolism, and is rescued by increasing metabolic flux. Moreover, DEC1 is needed to boost SC-islet maturity by synchronizing circadian glucose-responsive insulin secretion rhythms and clock machinery. Thus, DEC1 links circadian control to human β-cell maturation, highlighting its vitality to foster fully functional SC-islets.

## INTRODUCTION

The promise of broad cell therapy for diabetes has grown closer to reality with the advent of islet organoids grown from human pluripotent stem cells (SC-islets).[1-3] Islet transplants can cure insulin-dependent diabetics[4], but are limited by a scarcity of acceptable islets. SC-islets offer limitless cells for transplantation therapy, which can render human recipients free of daily insulin injections.[5,6] Yet, *in vitro* SC-islets are molecularly and functionally less mature than transplanted ones[7-9], and both lack the kinetics, precision, and magnitude of glucose-stimulated insulin secretion (GSIS) of adult islets.[10,11] This delays therapeutic benefit from SC-islet transplants, posing a key challenge to their broad application.

Mature islet function develops after birth, as hormone secretion capacity and the glucose threshold for secretion increase.[12-14] These changes are intertwined with the postnatal onset of islet circadian clocks.[15] The clock in islet β cells aligns GSIS responsiveness with the active phase of the day[16], likely to adapt to postnatal feeding-fasting rhythms.[8] Inactivating CLOCK or BMAL1—the master clock activators—renders mouse islets unable to mount mature GSIS responses, causing diabetes.[17-20] Whereas we find that inducing clock genes, via daily metabolic stimulation and recovery cycles, fosters mature function in human cadaveric/SC-islets by prompting circadian GSIS responses with a raised glucose threshold.[9] How the clock coordinates metabolic maturation of human β cells, however, remains poorly understood.[10,21]

To elucidate the regulation of human SC-β cell maturation by the circadian network, we focused on the transcription factor DEC1 (also called SHARP2, BHLHE40), as it partakes in the core regulatory circuit that defines human β-cell identity.[9] DEC1 entrains circadian rhythms to environmental cues, including light and feeding[22,23], by competing with CLOCK:BMAL1 for DNA E-box binding.[24] Recently, we found that DEC1 coordinates GSIS in mouse islets by synchronizing energy metabolism and exocytic gene rhythms, and *Dec1* knockout renders islets immature, causing lifelong glucose intolerance due to insufficient insulin responses.[25]

Here, we report that DEC1 is essential for SC-β cell maturation *in vitro* and *in vivo*. SC-islet organoids differentiate normally from *DEC1*-ablated human pluripotent stem cells (hPSCs) in scalable suspension culture[26], but exhibit impaired GSIS in both static and dynamic assays. RNA-seq of purified SC-β cells links this defect to downregulation of maturity-associated genes for glycolysis, mitochondrial respiration, and insulin exocytosis. Accordingly, *DEC1*$^{-/-}$ SC-islet organoids exhibit an energy deficit, prompted by lower glucose uptake, that hinders glycolysis and oxidative respiration and incites mitophagy. This renders *DEC1*$^{-/-}$ organoids unable to mature

even after transplantation into the kidney capsule of immunodeficient mice. We further find that DEC1 is required for enhancing SC-islet maturity through synchronization of circadian clock machinery and GSIS rhythms. Importantly, the GSIS deficit of *DEC1*$^{-/-}$ organoids can be rescued pharmacologically, by insulinotropic agents that bypass metabolism or increase metabolic flux. These findings establish DEC1 as a key link between the circadian clock and human β-cell metabolic maturation, highlighting the potential of leveraging circadian control to generate SC-islets with adult-like GSIS for improved transplantation therapy.

## RESULTS

### DEC1 is required for mature insulin responses to glucose in human SC-islets

To assess DEC1's role in human islet differentiation, we tracked its expression at each stage of our scalable protocol for differentiating 3D SC-islet organoids in suspension bioreactors (Figure 1A).[26] *DEC1* is minimally expressed in differentiating progenitors, but increases 12-fold in SC-islet β cells (Figure 1B). We thus disrupted *DEC1* in independent hPSC lines using an inducible CRISPR-Cas9 system (Figure S1A).[27] *DEC1*$^{-/-}$ lines differentiated normally and formed 3D SC-islet organoids with intact morphology, α and β cell composition, and insulin production (Figures S1C-S1G). We verified mRNA and protein loss throughout differentiation and *in vitro* maturation by extended culture (28 days) in serum-free media without added factors (Figures 1C, S1B, and S1F)[28,29]. DEC1 absence abolished induction of *IAPP,* a functional maturation marker for SC-β cells[28,30] (Figure 1D). Strikingly, *DEC1*$^{-/-}$ SC-islets show markedly diminished GSIS responses in both serial static and dynamic assays. Insulin secretion was significantly higher under static low (2.8mM) glucose incubations, while responses to saturating (20mM) glucose were impaired, despite normal insulin release upon subsequent chemical depolarization with KCl (Figure 1E).

Thus, *DEC1*$^{-/-}$ SC-islet organoids exhibit lower glucose threshold for insulin secretion and lower GSIS capacity—hallmarks of immature β-cell function.[12-14]

Longitudinal assays over four weeks of extended *in vitro* culture further revealed that *DEC1*$^{-/-}$ SC-islets fail to expand their GSIS capacity, as evidenced by consistently lower insulin secretion fold-change from 2.8mM to 20mM glucose (Figure 1F). In dynamic assays, although *DEC1*$^{-/-}$ SC-islets retain a biphasic pattern of insulin secretion, they show significantly reduced peak stimulation (4.14 ± 1.4-fold decrease) under saturating glucose, leading to diminished cumulative secretion (Figure 1G).

Collectively, these findings show that DEC1 is critical for refinement of GSIS responses during *in vitro* SC-islet maturation, including induction of maturity markers and elevation of the glucose threshold for insulin secretion and the GSIS capacity.

**DEC1 regulates β-cell maturity-linked effectors of glucose metabolism and insulin secretion**

To study DEC1's molecular role in SC-islet organoid maturation, we performed longitudinal RNA sequencing of *DEC1*$^{+/+}$ and *DEC1*$^{-/-}$ organoids at *in vitro* maturation days 7, 14, 21 and 28. 2,556 genes were differentially expressed, including suppression of *IAPP* and *SYT13*—an insulin secretory granule-resident protein required for insulin exocytosis (Figures S2A and S2B).[31] To investigate DEC1's role specifically in SC-β cells, we performed RNA sequencing in CD49a-purified cells from day 1 and 14 SC-islets (Figure S2C).[29] We identified a total of 2,622 genes significantly affected by *DEC1* ablation (Figures 2A and 2B). These comprise downregulated genes impacting β-cell function through roles as regulators or effectors of glucose import (*POU4F2*)[32], sensing (*HK2*)[33], glycolysis (*LDHB*)[34], mitochondrial oxidative phosphorylation (*NDUFA4*)[35], redox homeostasis (*TXNRD2*)[36,37], and insulin secretion (*ADCY5*)[38] (Figures 2C-F

and S2C-D). Genes upregulated in *DEC1*$^{-/-}$ SC-β cells, by contrast, include liver genes (*ALB, AFP*); disallowed glycolytic enzymes (*LDHA, PDK3*); mitochondrial depolarization (*TSPO*, *RACK1*)[39,40] and autophagy (*MMP9*, *BNIP3*)[41-44] machinery; and fatty acid metabolism enzymes (*ACSL1*, *ACSL6*, *ELOVL2*)[45-47] (Figures 2C-F and S2D). Notably, core circadian clock genes (*BMAL1, CLOCK*, *PER2*) lack differential expression (Figure 2B). Lastly, we confirmed these results by qPCR for a subset of genes (*LDHA, LDHB, HK2, SYT13, IAPP*, *GCK*) in enriched SC-β cells (Figure 2E).

Together, these findings implicate DEC1 in the control of GSIS through the regulation of glucose import and metabolism, mitochondrial integrity, and insulin release.

**DEC1 controls circadian insulin secretion and clock gene rhythms in human SC-islets**

The circadian clock attunes insulin secretion to daily feeding-fasting cycles[16] and is needed for mature β-cell function.[16,48] Previously, we reported that SC-islet organoids also display circadian GSIS responses.[9] Given DEC1's ability to entrain circadian rhythms to environmental cues[22,23], we investigated its requirement for GSIS rhythms. After synchronizing *DEC1*$^{+/+}$ and *DEC1*$^{-/-}$ SC-islets with forskolin[20,49], we performed sequential static GSIS and collected RNA for 24 hours (Figure 3A). *DEC1*$^{+/+}$ SC-islets showed circadian GSIS responses (p-value $< 0.05$ by JTK analysis) peaking at 36h after synchronization, with 2-fold greater responsiveness relative to mock treatment (Figures 3B and 3C). The increased GSIS responsiveness was driven by lower insulin secretion at basal (2.8mM) glucose stimulation, as seen before[9] (Figure S3A). Strikingly, *DEC1*$^{-/-}$ SC-islets failed to show circadian GSIS responses or a raised glucose threshold for secretion upon synchronization, with no improvement in GSIS responsiveness (Figures 3B, 3C, and S3A). We verified circadian *DEC1* expression in synchronized *DEC1*$^{+/+}$ SC-islets but not in

*DEC1*$^{-/-}$ or mock-treated *DEC1*$^{+/+}$ SC-islets (Figure 3D). We also validated antiphasic expression between the core circadian *CLOCK*/*BMAL1* activators and the *PER2* and *NR1D1* repressors in synchronized but not mock-treated *DEC1*$^{+/+}$ or *DEC1*$^{-/-}$ SC-islets (Figures 3E and S3B). Since *DEC1* regulates β-cell maturity and oxidative metabolism genes, we also examined expression patterns for *MAFA*, a key driver of mature β-cell physiology[50,51], and *DRP1,* which mediates mitochondrial fission under circadian control[52]. Remarkably, DEC1 loss abrogates circadian *MAFA* and *DRP1* expression (Figure 3E).

Together, these data demonstrate that DEC1 is essential for proper circadian rhythms in GSIS and in the expression of core clock and β cell maturity-linked genes.

**DEC1 sustains bioenergetics and mitochondrial integrity in maturing SC-β cells**

Given DEC1's role in regulating genes essential for respiration and redox homeostasis, we probed its influence on SC-β cell energetics and mitochondrial integrity. We find that DEC1$^{-/-}$ SC-β cells show diminished mitochondrial membrane potential, along with elevated mitophagy (Figure 4A), consistent with mitochondrial dysfunction[44,53,54]. Analyzing oxygen consumption rates in day 14 *DEC1*$^{-/-}$ SC-islet organoids reveals severely hindered basal, glucose-stimulated, ATP-linked, maximal, and non-mitochondrial respiration (Figures 4B, 4C, and S4A). Cellular reactive oxygen species levels are also significantly lower in *DEC1*$^{-/-}$ SC-β cells (Figure 4A), in line with diminished respiration. Thus, DEC1 is vital to bolster mitochondrial oxidative activity driving glucose-coupled energetics.

Reduced mitochondrial activity upon DEC1 loss could signal adaptations to reduced glucose utilization. Extracellular acidification rate analyses in day 14 SC-islet organoids reveal

that glycolysis and glycolytic capacity are indeed hampered by *DEC1* loss (Figures 4B-C, S4A). Further, we trace this deficit to stifled glucose import, as indicated by severely impaired uptake of a fluorescent glucose analogue in *DEC1*$^{-/-}$ SC-β cells (Figure 4A). Taken together with dulled glycolysis and mitochondrial oxidative activity[55], these data argue that DEC1 sustains proper glucose import and utilization, controlling the energy flux that underpins insulin secretion.

**A metabolic flux deficit underlies impaired insulin secretion upon DEC1 loss**

To test the extent to which the maturation defect of *DEC1*$^{-/-}$ organoids can be rescued by the *in vivo* milieu, we transplanted day 21 SC-islets under the kidney capsule of immunocompromised mice. Strikingly, *DEC1*$^{-/-}$ SC-islets show blunted GSIS responses compared to *DEC1*$^{+/+}$ SC-islets even after 21 weeks post-transplant (Figure 4D), as measured by insulin secretion following an intraperitoneal glucose injection. We thus conducted a targeted screen of insulinotropic agents to rescue the GSIS defect of *DEC1*$^{-/-}$ SC-islets *in vitro* (Figures 4E-G). Stimulation with forskolin, a cyclase agonist, failed to restore GSIS, suggesting defects in upstream steps. Ionomycin, a $Ca^{2+}$ ionophore, also failed to rescue GSIS, consistent with normal $Ca^{2+}$ influx dynamics in the absence of DEC1 (Figure S4B). Conversely, insulin secretion is restored to *DEC1*$^{+/+}$ levels by glucose-independent stimulation either with the diacylglycerol (DAG) mimetic phorbol 12-myristate 13-acetate (PMA), or with carbachol, a muscarinic receptor agonist (Figures 4E-G). We thus sought to rescue the glucose coupling defect of insulin secretion in *DEC1*$^{-/-}$ organoids by increasing metabolic flux. Raising the pyruvate pool, by inhibiting LDHA with oxamic acid and adding methyl-pyruvate, or the acetyl-CoA pool, by inhibiting PDK with DCA (dichloroacetate) successfully rescue GSIS (Figure 4F). Similarly, increasing glycolytic flux with dorzagliatin, a glucokinase activator, improved GSIS to *DEC1*$^{+/+}$ levels (Figure 4F). Metabolic flux increases

thus restore GSIS in *DEC1*$^{-/-}$ SC-islets, revealing a molecular mechanism for DEC1's role in coupling insulin secretion to glucose metabolism in mature β cells.

## DISCUSSION

Transplantable SC-islet organoids are likely to become a therapeutic option for severe insulin-dependent diabetes. Yet, human SC-islets transplants today exhibit delayed therapeutic benefit, with 4 months needed for >85% of recipients to reach <7% HbA1c levels[5], in contrast to 75 days or less for cadaveric islet transplants[56]. This delay likely reflects a need for SC-islets to complete functional maturation *in vivo*, in line with gradual molecular changes observed after transplant[9,57]. Common among these changes is the induction of circadian clock controllers[7,58], and we previously showed that recreating circadian rhythms *in vitro* enhances SC-islet maturity[9]. How the circadian clock coordinates SC-islet maturation, however, has remained elusive.

Here, we show that a circadian transcriptional regulator, DEC1 (SHARP2, BHLHE40), is vital for metabolic maturation of SC-β cells *in vitro* and *in vivo*. We previously predicted DEC1 to be the most interconnected transcription factor in the core regulatory circuit defining mature human β-cell identity[9]. Consistently, DEC1 is specifically induced in maturing SC-β cells, and its absence thwarts induction of maturity-linked gene circuits. The disrupted circuits control glucose import and metabolism, mitochondrial dynamics, and insulin exocytosis. Accordingly, *DEC1*$^{-/-}$ SC-islets show impaired glucose uptake, glycolysis, and oxidative metabolism. These changes stunt the ability of *DEC1*$^{-/-}$ organoids to mount circadian GSIS responses, which fail to mature even after *in vivo* transplant but are rescued by pharmacologically increasing metabolic flux. Thus, our findings demonstrate that DEC1 orchestrates coupling of insulin secretion to glucose sensing, linking the clock to acquisition of the mature β cell phenotype.

Our report of a circadian maturation factor offers a new paradigm for how the clock programs metabolic specialization. Mature β-cell physiology is thought to be orchestrated by the CLOCK/BMAL1 complex, as CLOCK or BMAL1 inactivation renders islets immature[17-19,59]. Yet three lines of evidence argue that such regulation is indirect. First, CLOCK and BMAL1 are already present early in human β-cell development, before maturation[60]. Second, they are not part of the core regulatory circuit of mature human β cells[9]. Third, we find here that *DEC1* loss suffices to render SC-islets immature, despite intact *CLOCK* and *BMAL1*. Our data thus support DEC1 as the direct arm of the clock imparting circadian GSIS control to drive β-cell maturation.

Mechanistically, our results indicate that DEC1 mediates maturation in SC-β cells by coordinating glucose utilization. DEC1-lacking β-cells exhibit reduced glucose influx and compensatory responses. These responses include induction of LDHA, which diverts pyruvate away from mitochondrial metabolism toward lactate production, and of lipid utilization genes, likely signaling a shift to alternative energy substrates. These adaptations recall the metabolic flexibility of neonatal β-cells, which lack strict glucose-dependence for insulin release and show higher lipid utilization[10,14,61]. Notably, stimulating glucose utilization via glucokinase activation rescues GSIS to wild-type SC-β cell levels, ruling out glycolytic defects.

DEC1's role in glucose metabolism is consistent with its ability to synchronize circadian rhythms with feeding[22,23]. Since islet circadian rhythms emerge postnatally[15], along with the onset of daily feeding-fasting, they likely foster maturation, at least in part, through DEC1-mediated optimization of glucose metabolism to daily energetics. We further found, in separate mouse studies[62], that DEC1 orchestrates mature GSIS responses by directly binding genes regulating integration of energy metabolism and insulin exocytosis to synchronize their expression, and thus energy and secretory rhythms. Taken together, our human and mouse

studies reveal a new, conserved mechanism whereby DEC1 links circadian clockwork to β-cell energetics and metabolic specialization.

How can DEC1's pathway be harnessed to improve SC-islet organoid maturity? Unlike global manipulation of metabolic cycles or the entire circadian network, precise tuning of DEC1 levels offers a new path to co-opt bioenergetic rhythms to control SC-β cell maturity. This may become possible by identifying DEC1's nutrient sensing mechanisms that could be targeted for external modulation. The persistent functional defect of transplanted *DEC1*$^{-/-}$ SC-islets suggests that such modulation would be relevant *in vivo*. Thus, further delineating how the circadian system underpins SC-β cell maturity heralds new avenues to attain fully functional SC-islets to improve islet replacement therapies.

**ACKNOWLEDGEMENTS**

We thank Douglas A. Melton for support during the initial stage of this project; the University of Pennsylvania Diabetes Research Center Islet Cell Biology Core for technical support and critical discussions; and Israeli M. Galicia-Silva, Samuel D. Pollock, Niloo Rasouli and members of the Alvarez-Dominguez laboratory for critical feedback on this manuscript. This work was supported by grants to Sam Preza and J.R.A-D. from the Howard Hughes Medical Institute through the Gilliam Fellows Program, the NIH (K01DK129442), NIH/NIDDK 1DP1DK130673, the Human Islet Research Network (U24DK104162), start-up funding from the Perelman School of Medicine at the University of Pennsylvania, and by a pilot award from the Diabetes Research Center at the University of Pennsylvania (P30DK19525) to J.R.A-D., who was also supported by a Howard Hughes Medical Institute Life Sciences Research Foundation Fellowship; and by

grants to Douglas A. Melton from the JDRF (5-COE-2020-967-M-N), and the JPB Foundation (award no. 1094).

## AUTHOR CONTRIBUTIONS

S.P., B.Z., Z.G., M.L., A.B., and J.RA.-D. performed experiments. S.P., M.L., and A.B. conducted bioinformatics analyses. S.P., Z.G., and J.RA.-D. designed the research and interpreted results. S.P., B.Z., Z.G., A.B., and J.RA.-D. wrote the manuscript.

## DECLARATION OF INTERESTS

The authors declare that they have no competing interests.

## RESOURCE AVAILABILITY

### Lead Contact and Materials Availability

Further information and requests for resources and reagents should be directed to the Lead Contact, Juan R. Alvarez-Dominguez (Juan.Alvarez@pennmedicine.upenn.edu). All unique/stable reagents generated in this study are available from the Lead Contact with a completed Materials Transfer Agreement.

## EXPERIMENTAL MODEL AND SUBJECT DETAILS

### Human cell lines

The HUES8 (NIH hESC registry #09-0021; male) line was used for directed differentiation, and lines derived from HUES8 were used for CRISPR/Cas9 genome editing followed by directed

differentiation. Undifferentiated cells were maintained as aggregates in supplemented mTeSR1 medium (StemCell Technologies) using spinner flasks (Corning) set at a 70rpm rotation rate in a 37°C 5%CO2 incubator.

## STAR METHODS

### SC-islet differentiation in 3D suspension culture

Directed differentiation of human pluripotent stem cells into pancreatic islets was performed as previously described in 30-mL stirred suspension bioreactors (REPROCELL; ABBWVS03).[26] All experiments were conducted using the HUES 8 (NIH registry #NIHhESC-09-0021) line maintained in mTeSR1 (StemCell Technologies, 85850) media on a rotator stir plate (Chemglass) at 70 RPM in a humidified 37°C, 5% $CO_2$ tissue culture incubator. Maintenance cultures were passaged every 3 days using a sequential filtration approach: 300 µm strainers were used to remove large aggregates, followed by 37 µm strainers (StemCell Technologies, 27250) to eliminate small debris. Cells were then incubated with Gentle Cell Dissociation Reagent (GCDR, StemCell Technologies, 100-0485) for 6 minutes, counted for viability, and reseeded at $0.6 \times 10^6$ cells/mL in mTeSR1 supplemented with 10 µM ROCK inhibitor (Y27632, Abcam). Cells underwent at least three passages after thaw from cryopreservation before differentiation, with each passage achieving a minimum threefold expansion. A six-stage differentiation protocol was used to generate SC-islets. Cells were seeded at $0.6 \times 10^6$ cells/mL in mTeSR1 with Y27632 on day 0, typically using 18M cells in 30 mL total volume. A half-media change was performed at 24 hours, replacing with fresh mTeSR1 (without Y27632), followed by a full media change on day 2. Differentiation was initiated on day 3 (Stage 1) and proceeded through Stage 6, with media changes performed on a 24-hour feeding cycle as described[26].

**Reverse transcription-quantitative PCR (RT-qPCR)**

RNA extraction and purification was done using the DirectZol RNA miniPrep (Zymo Research, R2050), which included a DNase treatment to eliminate genomic DNA contamination. Complementary DNA (cDNA) synthesis was carried out using the High-Capacity cDNA reverse transcription kit (Invitrogen, 18080051), according to manufacturer instructions. qPCR reactions were performed using SYBR green master mix (Applied biosystems, A25742) on a StepOnePlus Real-Time PCR system (Applied biosystems). All reactions were done in triplicate, and melting curves were run to establish specificity of amplification. The primer sequences used for amplification are listed in the Resources Table.

**Static glucose-stimulated insulin secretion**

Static glucose-stimulated insulin secretion (GSIS) assays were performed on Stage 6 clusters[26]. Clusters were first washed and equilibrated in KREBs buffer (128 mM NaCl, 5 mM KCl, 2.7 mM CaCl2, 1.2 mM MgSO4, 1 mM Na2HPO4, 1.2 mM KH2PO4, 5 mM NaHCO3, 10 mM HEPES, 0.1% BSA) containing 2.8 mM glucose for 1 hour. Then, we used 12 µm polycarbonate Millicell inserts (Sigma-Aldrich, PIXP01250) in 24-well plates to sequentially incubate clusters in low glucose (2.8 mM, 1 hour), high glucose (20 mM, 1 hour), and KCl (30 mM in 2.8 mM glucose, 1 hour). Media samples were collected after each incubation period. Following the assay, clusters were dispersed into single cells using TrypLE (Fisher Scientific, 50-591-419), which were counted to normalize secretion data. Insulin concentrations in the collected samples were measured using an ultrasensitive human insulin ELISA (ALPCO, 80-INSHUU-E01.1), with results expressed as µIU/mL/1000 cells. For insulin content measurements, cluster lysates were

prepared using M-PER (Thermo Fisher, 78501) and analyzed using the same ELISA protocol. All assays were performed in triplicate.

**Dynamic glucose-stimulated insulin secretion**

Dynamic glucose-stimulated insulin secretion assays were conducted using an automated perifusion system (BioRep). Size-matched islets were carefully selected and placed in perifusion chambers. The chambers were first equilibrated with KREBs buffer containing basal glucose (2.8 mM) for 60 minutes at a constant flow rate of 100 µL/min. Following equilibration, islets were sequentially exposed to low glucose (2.8 mM) for 16 minutes, then high glucose (20 mM) for 32 minutes. For dynamic GSIS with insulinotropic agent, (10µM) PMA an additional 20 mM glucose step incorporating PMA was done for 16 minutes, followed by 16 minutes 2.8mM glucose, and 16 minutes of 2.8 mM glucose + 30 mM KCl. Insulin secretion data were normalized to the mean insulin release during the initial basal incubation.

**Flow cytometry for differentiation cell markers**

Suspension culture Samples were treated with TrypLE to dissociate clusters to single cells, which were then fixed in 4% Paraformaldehyde for 30 minutes at 4°C. The fixed cells were then blocked at 4°C for 30 minutes in a blocking buffer (5% Donkey serum [Jackson Immunoresearch], 0.1% Saponin [Sigma Aldrich] in PBS) to permeabilize cell membranes and minimize nonspecific binding. Primary antibody incubations were conducted overnight at 4°C, with antibodies selected based on the differentiation stage of the cells. The following day samples were incubated at room temperature for 1 hour with the appropriate fluorophore-conjugated secondary antibodies. The cells were resuspended in a washing buffer (5% donkey

serum, PBS) and analyzed using an Accuri C6 Plus flow cytometer (BD Biosciences). Data acquisition and analysis was performed using FlowJo software. The antibodies used are listed in Resource Table and are as previously reported.[26]

**Immunofluorescence Staining**

Measurements were performed based on previously established protocols.[9,26] SC-islet organoids were collected and fixed in 4% paraformaldehyde for 15 minutes at room temperature and washed with PBS. After fixation organoids were resuspended in embedding gel (2.5% agar, 2.5% gelatin). A droplet of the solution was transferred into an embedding cassette, stored in 70% ethanol, and then submitted to the University of Pennsylvania Pathology and Imaging Core (RRID: SCR_022420) for paraffin embedding. For deparaffinization the slides were treated with xylene, followed by serial ethanol and water washes. Antigen retrieval was done by incubating the slides in warm 1X Citrate buffer (Sigma Aldrich, C9999-1000ML) using a crockpot water bath at "high" temperature for 5 minutes and then "warm" for 30 minutes. The slides were subsequently blocked and permeabilized using a blocking buffer consisting of 5% donkey serum, 0.3% Triton and PBS solution for 1 hour to minimize nonspecific binding. Primary antibody staining was conducted overnight in 4°C for C-PEPTIDE and DEC1 (Resource Table). After incubation with primary antibodies the slides were incubated with the appropriate secondary antibodies for an hour at room temperature and then counterstained with DAPI (Thermo Fisher, P36935). After staining, fluorescent imaging was performed using a fluorescent microscope.

**SC-β cell enrichment with CD49a**

Fluorescence-activated cell sorting (FACS) was performed as previously reported[29] to isolate live, marker-defined β-cell populations from Stage 6 cultures. Cells were first dissociated into a single-cell suspension using TrypLE enzymatic digestion. Aggregates were dispersed mechanically through repeated pipetting with a P1000 micropipette, ensuring uniform suspension while minimizing cellular stress. The digestion reaction was quenched with S3 medium, followed by centrifugation at 300 × g for 5 minutes. The pellet was resuspended in sorting buffer (PBS + 1% BSA + 2 mM EDTA), filtered through a 35 µm strainer, and counted to determine cell concentration. For immunostaining, cells were aliquoted at $10 \times 10^6$ cells/mL and incubated with anti-human CD49a-PE (1:11 dilution) (Miltenyi Biotec, 130-101-397) antibody for 20 minutes at room temperature, protected from light with gentle agitation every 3–4 minutes. These markers were selected to enrich for pancreatic β-cells within the heterogenous Stage 6 population. After incubation, cells were washed twice by centrifugation (300 × g, 5 minutes) and resuspended in sorting buffer at a final concentration of $10 \times 10^6$ cells/mL. FACS sorting was performed using a 100 µm nozzle at a rate of ~10,000 events per second. $CD49a^+$ cells were selectively sorted to enrich for insulin-producing β-cells within the Stage 6 population. Cells were collected into FACS tubes containing 1 mL sorting buffer supplemented with 1:1000 ROCK inhibitor (Y27632) to enhance post-sort survival. Sorted β-cells were kept on ice and subsequently transferred to pre-warmed media for further functional characterization or RNA extraction for downstream RNA-sequencing.

**RNA-sequencing and differential gene expression**

RNA-sequencing was performed as previously described[9]. RNA from CD49a enriched SC-β cells (~300k cells) or SC-islets (~300k cells) was isolated for RNA-sequencing. Sequenced

reads were STAR[56] aligned using default parameters. Read counts per gene were quantified using HTSeq[57] and normalized using DESeq[58]. The expression levels were normalized to counts per million (CPM), with genes considered expressed if CPM was greater than 1.

**Gene set enrichment analysis**

Gene lists ranked by $\log_2$fold change (*DEC1*$^{-/-}$/*DEC1*$^{+/+}$) were analyzed for enrichment of genes using GSEA[59] with default parameters and "-metric log2_Ratio_of_Classes." Pathway annotations were derived from Hallmark and C5 (Gene Ontology) databases to investigate the overrepresentation of curated pathways and biological processes.

**Forskolin synchronization experiments**

Forskolin was used to synchronize circadian rhythms[20,49] prior to downstream assays. Stage 6 SC-islet organoids were incubated in Stage 3 media supplemented with 10µM forskolin (Stemgent, 04-0025) for 1 hour. Following the 1-hour forskolin shock, SC-islets were returned to culture and allowed to recover in fresh Stage 3 media for an additional 15 hours. After the 15-hour post-shock incubation period, SC-islets were harvested for downstream analyses including static GSIS and RT-qPCR. Insulin secretion fold changes and relative expression of genes of interest were analyzed by JTK_CYCLE[60] analysis using Nitecap[61], which employs nonparametric rank-based testing to detect periodic signals by comparing time-series data against idealized sinusoidal waveforms. Rhythmicity significance was assessed by fitting the data to models with varying periods, generating p-values and estimating peak phase (lag) in a 24h cycle. The MetaCycle meta2d() function was used with default parameters to calculate rhythmicity metrics, including Benjamini-Hochberg corrected p-values and phase estimates. For

visualization, time-series data were detrended by subtracting a linear regression fit while maintaining relative scaling proportions by considering the means and SEMs of both genotypes.

**Cellular and mitochondrial energetics analysis**

Flow cytometry analyses of mitochondrial autophagy, mitochondrial membrane potential, cellular reactive oxygen species, and glucose analogue uptake were conducted in day 14 SC-islet organoids. Clusters were dissociated into single-cell suspensions using TrypLE and resuspended in Stage 3 media. Single-cell suspensions were incubated with a freshly prepared staining solution containing 50nM TMRE (Abcam; ab113852), 5µM CellROX Deep Red (Invitrogen, C10422), 20µM 2-NBDG (Thermo Fisher, N13195), or 100nM Mtphagy dye (Dojindo, Mt048) in Stage 3 medium. CD49a antibody (1:50) was included during incubation to gate-select for SC-β cells. Cells were incubated at 37°C for 30 minutes in a humidified 5% $CO_2$ incubator. After staining, cells were washed twice with 1% BSA in PBS and filtered through a 35 µm nylon mesh into flow cytometry tubes (STELLAR SCIENTIFIC, FSC-9005). Flow cytometry data was acquired using a BD Accuri C6 Plus flow cytometer (BD Biosciences) and analyzed using FlowJo v10.8.1 (BD Life Sciences). Fluorescence intensities were normalized to unstained controls and data were gated based on forward and side cell scatter parameters to exclude debris and doublets.

**Metabolic flux analysis**

Oxygen consumption rate (OCR) measurements were performed using the Seahorse XFe96 Analyzer and Spheroid FluxPak (Agilent, 102905-100) to assess mitochondrial function in SC-islets at day 14 of *in vitro* maturation. One day prior to the assay, sensor cartridge wells were

hydrated by incubating with 200 µL of Seahorse calibrant solution (Agilent) at 37°C overnight in a non-$CO_2$ incubator. Spheroid plate wells were coated with 30 µL of 100 ng/mL poly-D-lysine (Sigma, P7280). Injection basal media (Agilent; 103335-100), wash media (basal media with 0.5% FBS), and assay media (basal media with 0.5% FBS and 1mM glucose) were freshly prepared and stored at 4°C protected from light. On the day of the experiment, all media were adjusted to pH 7.4 and warmed and kept at 37°C. SC-islets were hand-selected and washed twice in wash for 15 minutes at room temperature. After washing, 8-10 size-matched SC-islets were transferred per well in a total volume of 30 µL using an islet-loading mold and gently overlaid with 175 µL of pre-warmed assay media. The Spheroid plate was incubated for 1 hour at 37°C in a $CO_2$-free incubator to allow for metabolic equilibration. Prior to the assay, the sensor cartridge was calibrated on the Seahorse XFe96 Analyzer for 15 minutes. Mitochondrial stress testing was then performed by sequential injection of 20 µL the following compounds, prepared in injection basal media and loaded into the cartridge injection ports: 20 mM glucose with 0.5mM glutamine and 3.5mM amino acid mix, 5 µM oligomycin (Sigma, O4876), 2 µM FCCP (Sigma, C2920), and a combination of 5 µM rotenone (Sigma, 557368) and 5 µM antimycin A (Sigma, A8674). Assay cycles consisted of 2 minutes of mixing followed by 3 minutes of measurement. The number of cycles performed was as follows: 6 for basal OCR, 4 for 20 mM glucose with 0.5mM glutamine and 3.5mM amino acid mix, 5 for oligomycin, 4 for FCCP, and 6 for rotenone + antimycin A.

**Transplantation studies**

Transplantation of SC-islets under the kidney capsule of 8-12 week-old immunodeficient SCID-beige mice was done as previously described.[9] SC-islets were washed and resuspended in RPMI

and submitted to University of Pennsylvania Stem Cell and Xenograft Core (SCXC – PRID: SCR_010035). The procedure was performed under anesthesia. Post-surgery, mice were monitored for pain and distress, with symptomatic mice isolated and observed for two days. If conditions did not improve, euthanasia was performed.

**Insulinotropic agents screen**

SC-islets were prepared and incubated in 2.8mM glucose KREBs buffer in typical static GSIS fashion. Insulinotropic agents were added to KREBs buffer during the high glucose (20 mM glucose) 1h incubation step at 37°C in a humidified 5% $CO_2$ incubator. The following compounds were used: dorzagliatin (10µM) (Selleckchem, S6921), forskolin (10 µM) (Stemolecule, 04-0025), PMA (10µM) (Santa Cruz Biotechnology, SC-3576B), ionomycin (10µM) (StemCell Technologies, 73722), and carbachol (1mM) (Santa Cruz Biotechnology, SC-202092). For select metabolic flux modulators, longer pre-incubation was required: cells were treated with either 1 mM dichloroacetate (DCA) (Selleckchem, S8615) or 1 mM oxamate (MedChemExpress, HY-W013032A) for 24 hours prior to GSIS. For oxamate-treated samples, 100µM methyl pyruvate (Sigma Aldrich, 371173) was also added during the 1-hour high-glucose stimulation step only. Following treatment, GSIS was performed as described above. Media samples were collected for insulin quantification, and data were normalized to cell counts.

**Calcium influx**

SC-islets were washed twice, followed by staining with 16.7µM Fura2-AM (Life Technologies; F- F1225) in Krebs buffer supplemented with 5mM glucose for 45 minutes at 37°C. Islets were then transferred to a perifusion chamber on a homeothermic platform, perifused with 37°C Krebs

buffer at a flow rate of 1mL/min. and imaged with an inverted Zeiss microscope (Axio Observer.Z1). After imaging in the absence of substrate, a physiological amino acids mixture (0.5 mM glutamine and 3.5mM amino acid mix) alone and with increasing glucose levels (3mM, 16.7mM) were sequentially applied, followed by washing all substrates away and applying KCl (30mM). Intracellular $Ca^{2+}$ was measured by dual-wavelength fluorescence microscopy using the Zeiss AxioVision system.

**Resource Table**

| **Antibodies** | | |
|---|---|---|
| Reagent | Source | Identifier |
| Rat anti-C-Peptide | Iowa DSHB | Cat# GN-ID4 |
| PE anti-CD49a | Miltenyi Biotec | Cat# 130-101-397 |
| Mouse anti-NKX6.1 | Iowa DSHB | Cat# F55A12 |
| Rabbit anti-Glucagon | Cell signaling technologies | Cat# D16G10 |
| Goat anti-Pdx1 | R & D systems | Cat# AF2419 |
| Mouse anti-Glucagon | Santa Cruz | Cat# SC-514592 |
| Rabbit anti-DEC1 | Novus Biologicals | Cat# NB100-1800 |
| Goat anti-Sox17 | R & D systems | Cat# AF1924 |
| Rabbit anti-Ki67 | Abcam | Cat# ab16667 |

| | | |
|---|---|---|
| Rabbit anti-Chromogranin-A | Abcam | Cat# ab15160 |
| Donkey anti-Rat IgG, Alexa Fluor™ 488 | Invitrogen | Cat# A-21208 |
| Donkey anti-Rabbit IgG, Alexa Fluor™ 647 | Invitrogen | Cat# A-31573 |
| Donkey anti-Mouse IgG, Alexa Fluor™ 647 | Invitrogen | Cat# A-31571 |
| Donkey anti-Rabbit IgG, Alexa Fluor™ 488 | Invitrogen | Cat# R37118 |
| Donkey anti-Goat IgG, DyLight™ 488 | Invitrogen | Cat# SA5-10086 |

| **Oligonucleotides (RT-qPCR)** | |
|---|---|
| Gene | Sequence |
| h18s | F: cgcagctaggaataatggaatagg,<br>R: catggcctcagttccgaaa |
| hMAFA | F: gcttcagcaaggaggaggtcat,<br>R: tctggagttggcacttctcgct |
| hIAPP | F: agcggaaatgcaacactgccac |

| | |
|---|---|
| | R: cgttggtagatgagagaatggca |
| hCLOCK | F: CAGGCAGCATTTACCAGCTCATG |
| | R: GTAGCTTGAGACATCACTGGCTG |
| hPER2 | F: AGCTGCTTGGACAGCGTCATCA |
| | R: CCTTCCGCTTATCACTGGACCT |
| hNR1D1 | F: CTGCCAGCAATGTCGCTTCAAG |
| | R: TGGCTGCTCAACTGGTTGTTGG |
| hHK2 | F: GAGTTTGACCTGGATGTGGTTGC |
| | R: CCTCCATGTAGCAGGCATTGCT |
| hLDHA | F: GGATCTCCAACATGGCAGCCTT |
| | R: AGACGGCTTTCTCCCTCTTGCT |
| hLDHB | F: GGACAAGTTGGTATGGCGTGTG |
| | R: AAGCTCCCATGCTGCAGATCCA |
| hSYT13 | F: TCAAGAGGCAGGTCACAGAGGA |
| | R: CCTTCTGACAGTCATAGTCCAGG |
| hGCK | F: CATCTCCGACTTCCTGGACAAG |
| | R: TGGTCCAGTTGAGAAGGATGCC |
| hSHARP2 | F: taaagcggagcgaggacagcaa |
| | R:gatgttcgggtaggagatccttc |

| | |
|---|---|
| hBMAL1 | F: gctcaggagaacccaggttatc |
| | R: gcatctgcttccaagaggctca |
| hDRP1 | F: gatgccatagttgaagtggtgac |
| | R: ccacaagcatcagcaaagtctgg |
| **Oligonucleotides for PCR** | |
| SHARP2_sgRNA1 Flanking PCR Primers | F: CCCAACTGAAGCTGCATCTC |
| | R: GCACTCGTTAATCCGGTCAC |
| SHARP2_sgRNA2 Flanking PCR Primers | F: GAAAGGGCAGACGATGGTTC |
| | R: TGTGTGTTTCTTGGCGTGTT |
| **Oligonucleotides for Sanger Sequencing** | |
| SHARP2_sgRNA1 | TGTTATGCGCCACTCTCAAC |
| SHARP2_sgRNA2 | CGTCTTGCAGGAGACCTACA |
| **Oligonucleotides** (CRISPR sgRNA) | |
| SHARP2_CRISPR_sgRNA1 | taatacgactcactataggg gaaagaaaccccagcctctg gttttagagctagaaatagcaagttaaaataaggctagtccgttatcaacttgaaaaagt ggcaccgagtcggtgctttt |

| | |
|---|---|
| SHARP2_CRISPR_sgRNA2 | taatacgactcactataggg gcgctgcggagggagtcgcc gttttagagctagaaatagcaagttaaaataaggctagtccgttatcaacttgaaaaagt ggcaccgagtcggtgctttt |
| *F: Forward Strand<br>*R: Reverse Strand | |
| **Software and Algorithms** | |
| BEDTools | https://bedtools.readthedocs.io/en/latest/ |
| R v2022.12.0+353 | R Core Team |
| Nitecap | https://nitecap.org/ |

## QUANTIFICATION AND STATISTICAL ANALYSIS

No statistical methods were used to predetermine sample size or remove outliers. To assess the statistical difference between two sets of unpaired data, GraphPad Prism was used to calculate statistical significance for all non-RNA sequencing data. To assess the statistical difference between two sets of unpaired, the Shapiro-Wilk normality test was first performed as column or grouped analysis. A two-sided unpaired t-test was then used to assess confidence on the measured difference of their mean values. For unpaired data that did not follow a normal distribution, we used a non-parametric Wilcoxon rank sum test to determine if they belong to the same parent distribution.

## EXCEL TABLE TITLE AND LEGENDS

**Table S1. SC-β cells differential gene expression output by DESeq. Related to Figure 2.**

**Table S2. Gene ontology from GSEA analysis. Related to Figure 2.**

**Table S3. SC-islets differential gene expression output by DESeq. Related to Figure S2.**

## REFERENCES


1. Melton, D. (2021). The promise of stem cell-derived islet replacement therapy. Diabetologia *64*, 1030-1036. 10.1007/s00125-020-05367-2.
2. Sneddon, J.B., Tang, Q., Stock, P., Bluestone, J.A., Roy, S., Desai, T., and Hebrok, M. (2018). Stem Cell Therapies for Treating Diabetes: Progress and Remaining Challenges. Cell Stem Cell *22*, 810-823. 10.1016/j.stem.2018.05.016.
3. Hogrebe, N.J., Ishahak, M., and Millman, J.R. (2023). Developments in stem cell-derived islet replacement therapy for treating type 1 diabetes. Cell Stem Cell *30*, 530-548. 10.1016/j.stem.2023.04.002.
4. Verhoeff, K., Marfil-Garza, B.A., and Shapiro, A.M.J. (2021). Update on islet cell transplantation. Curr Opin Organ Transplant *26*, 397-404. 10.1097/MOT.0000000000000891.
5. REICHMAN, T.W., RICORDI, C., NAJI, A., MARKMANN, J.F., PERKINS, B.A., WIJKSTROM, M., PARASKEVAS, S., BRUINSMA, B., MARIGOWDA, G., SHIH, J.L., et al. (2023). 836-P: Glucose-Dependent Insulin Production and Insulin-Independence in Type 1 Diabetes from Stem Cell–Derived, Fully Differentiated Islet Cells—Updated Data from the VX-880 Clinical Trial. Diabetes *72*. 10.2337/db23-836-P.
6. Wang, S., Du, Y., Zhang, B., Meng, G., Liu, Z., Liew, S.Y., Liang, R., Zhang, Z., Cai, X., Wu, S., et al. (2024). Transplantation of chemically induced pluripotent stem-cell-derived islets under abdominal anterior rectus sheath in a type 1 diabetes patient. Cell *187*, 6152-6164 e6118. 10.1016/j.cell.2024.09.004.
7. Augsornworawat, P., Hogrebe, N.J., Ishahak, M., Schmidt, M.D., Marquez, E., Maestas, M.M., Veronese-Paniagua, D.A., Gale, S.E., Miller, J.R., Velazco-Cruz, L., and Millman, J.R. (2023). Single-nucleus multi-omics of human stem cell-derived islets identifies deficiencies in lineage specification. Nat Cell Biol *25*, 904-916. 10.1038/s41556-023-01150-8.
8. Helman, A., Cangelosi, A.L., Davis, J.C., Pham, Q., Rothman, A., Faust, A.L., Straubhaar, J.R., Sabatini, D.M., and Melton, D.A. (2020). A Nutrient-Sensing Transition at Birth Triggers Glucose-Responsive Insulin Secretion. Cell Metab *31*, 1004-1016 e1005. 10.1016/j.cmet.2020.04.004.
9. Alvarez-Dominguez, J.R., Donaghey, J., Rasouli, N., Kenty, J.H.R., Helman, A., Charlton, J., Straubhaar, J.R., Meissner, A., and Melton, D.A. (2020). Circadian Entrainment Triggers Maturation of Human In Vitro Islets. Cell Stem Cell *26*, 108-122 e110. 10.1016/j.stem.2019.11.011.
10. Barsby, T., and Otonkoski, T. (2022). Maturation of beta cells: lessons from in vivo and in vitro models. Diabetologia *65*, 917-930. 10.1007/s00125-022-05672-y.
11. Kaestner, K.H., Campbell-Thompson, M., Dor, Y., Gill, R.G., Glaser, B., Kim, S.K., Sander, M., Stabler, C., Stewart, A.F., and Powers, A.C. (2021). What is a beta cell? - Chapter I in the Human Islet Research Network (HIRN) review series. Mol Metab *53*, 101323. 10.1016/j.molmet.2021.101323.
12. Aguayo-Mazzucato, C., Sanchez-Soto, C., Godinez-Puig, V., Gutierrez-Ospina, G., and Hiriart, M. (2006). Restructuring of pancreatic islets and insulin secretion in a postnatal critical window. PLoS One *1*, e35. 10.1371/journal.pone.0000035.

13. Blum, B., Hrvatin, S., Schuetz, C., Bonal, C., Rezania, A., and Melton, D.A. (2012). Functional beta-cell maturation is marked by an increased glucose threshold and by expression of urocortin 3. Nat Biotechnol *30*, 261-264. 10.1038/nbt.2141.
14. Stolovich-Rain, M., Enk, J., Vikesa, J., Nielsen, F.C., Saada, A., Glaser, B., and Dor, Y. (2015). Weaning triggers a maturation step of pancreatic beta cells. Dev Cell *32*, 535-545. 10.1016/j.devcel.2015.01.002.
15. Rakshit, K., Qian, J., Gaonkar, K.S., Dhawan, S., Colwell, C.S., and Matveyenko, A.V. (2018). Postnatal Ontogenesis of the Islet Circadian Clock Plays a Contributory Role in beta-Cell Maturation Process. Diabetes *67*, 911-922. 10.2337/db17-0850.
16. Bass, J., and Takahashi, J.S. (2010). Circadian integration of metabolism and energetics. Science *330*, 1349-1354. 10.1126/science.1195027.
17. Perelis, M., Ramsey, K.M., Marcheva, B., and Bass, J. (2016). Circadian Transcription from Beta Cell Function to Diabetes Pathophysiology. J Biol Rhythms *31*, 323-336. 10.1177/0748730416656949.
18. Sadacca, L.A., Lamia, K.A., deLemos, A.S., Blum, B., and Weitz, C.J. (2011). An intrinsic circadian clock of the pancreas is required for normal insulin release and glucose homeostasis in mice. Diabetologia *54*, 120-124. 10.1007/s00125-010-1920-8.
19. Lee, J., Kim, M.S., Li, R., Liu, V.Y., Fu, L., Moore, D.D., Ma, K., and Yechoor, V.K. (2011). Loss of Bmal1 leads to uncoupling and impaired glucose-stimulated insulin secretion in beta-cells. Islets *3*, 381-388. 10.4161/isl.3.6.18157.
20. Marcheva, B., Ramsey, K.M., Buhr, E.D., Kobayashi, Y., Su, H., Ko, C.H., Ivanova, G., Omura, C., Mo, S., Vitaterna, M.H., et al. (2010). Disruption of the clock components CLOCK and BMAL1 leads to hypoinsulinaemia and diabetes. Nature *466*, 627-631. 10.1038/nature09253.
21. Wortham, M., and Sander, M. (2021). Transcriptional mechanisms of pancreatic beta-cell maturation and functional adaptation. Trends Endocrinol Metab *32*, 474-487. 10.1016/j.tem.2021.04.011.
22. Sato, F., Kohsaka, A., Bhawal, U.K., and Muragaki, Y. (2018). Potential Roles of Dec and Bmal1 Genes in Interconnecting Circadian Clock and Energy Metabolism. Int J Mol Sci *19*. 10.3390/ijms19030781.
23. Kato, Y., Kawamoto, T., Fujimoto, K., and Noshiro, M. (2014). DEC1/STRA13/SHARP2 and DEC2/SHARP1 coordinate physiological processes, including circadian rhythms in response to environmental stimuli. Curr Top Dev Biol *110*, 339-372. 10.1016/B978-0-12-405943-6.00010-5.
24. Honma, S., Kawamoto, T., Takagi, Y., Fujimoto, K., Sato, F., Noshiro, M., Kato, Y., and Honma, K. (2002). Dec1 and Dec2 are regulators of the mammalian molecular clock. Nature *419*, 841-844. 10.1038/nature01123.
25. Montalvo, A.P., Gruskin, Z.L., Leduc, A., Liu, M., Gao, Z., Ahn, J.H., Straubhaar, J.R., Slavov, N., and Alvarez-Dominguez, J.R. (2023). An adult clock component links circadian rhythms to pancreatic β-cell maturation. bioRxiv, 2023.2008.2011.552890. 10.1101/2023.08.11.552890.
26. Pollock, S.D., Galicia-Silva, I.M., Liu, M., Gruskin, Z.L., and Alvarez-Dominguez, J.R. (2023). Scalable generation of 3D pancreatic islet organoids from human

pluripotent stem cells in suspension bioreactors. STAR Protoc *4*, 102580. 10.1016/j.xpro.2023.102580.
27. Gonzalez, F., Zhu, Z., Shi, Z.D., Lelli, K., Verma, N., Li, Q.V., and Huangfu, D. (2014). An iCRISPR platform for rapid, multiplexable, and inducible genome editing in human pluripotent stem cells. Cell Stem Cell *15*, 215-226. 10.1016/j.stem.2014.05.018.
28. Velazco-Cruz, L., Song, J., Maxwell, K.G., Goedegebuure, M.M., Augsornworawat, P., Hogrebe, N.J., and Millman, J.R. (2019). Acquisition of Dynamic Function in Human Stem Cell-Derived beta Cells. Stem Cell Reports *12*, 351-365. 10.1016/j.stemcr.2018.12.012.
29. Veres, A., Faust, A.L., Bushnell, H.L., Engquist, E.N., Kenty, J.H., Harb, G., Poh, Y.C., Sintov, E., Gurtler, M., Pagliuca, F.W., et al. (2019). Charting cellular identity during human in vitro beta-cell differentiation. Nature *569*, 368-373. 10.1038/s41586-019-1168-5.
30. Davis, J.C., Ryaboshapkina, M., Kenty, J.H., Eser, P.O., Menon, S., Tyrberg, B., and Melton, D.A. (2024). IAPP Marks Mono-hormonal Stem-cell Derived beta Cells that Maintain Stable Insulin Production in vitro and in vivo. bioRxiv. 10.1101/2024.04.10.587726.
31. Norris, N., Yau, B., Famularo, C., Webster, H., Loudovaris, T., Thomas, H.E., Larance, M., Senior, A.M., and Kebede, M.A. (2024). Optimized Proteomic Analysis of Insulin Granules From MIN6 Cells Identifies Scamp3, a Novel Regulator of Insulin Secretion and Content. Diabetes *73*, 2045-2054. 10.2337/db24-0355.
32. Bitsi, S., Ali, H., Maskell, L., Ounzain, S., Mohamed-Ali, V., and Budhram-Mahadeo, V.S. (2016). Profound hyperglycemia in knockout mutant mice identifies novel function for POU4F2/Brn-3b in regulating metabolic processes. Am J Physiol Endocrinol Metab *310*, E303-312. 10.1152/ajpendo.00211.2015.
33. Roberts, D.J., and Miyamoto, S. (2015). Hexokinase II integrates energy metabolism and cellular protection: Akting on mitochondria and TORCing to autophagy. Cell Death & Differentiation *22*, 248-257. 10.1038/cdd.2014.173.
34. Fu, A. (2024). Reconsidering lactate disallowance in pancreatic beta cells. Trends Endocrinol Metab *35*, 1023-1025. 10.1016/j.tem.2024.06.014.
35. Yagil, C., Varadi-Levi, R., and Yagil, Y. (2018). A novel mutation in the NADH dehydrogenase (ubiquinone) 1 alpha subcomplex 4 (Ndufa4) gene links mitochondrial dysfunction to the development of diabetes in a rodent model. Dis Model Mech *11*. 10.1242/dmm.036699.
36. Stancill, J.S., and Corbett, J.A. (2023). Hydrogen peroxide detoxification through the peroxiredoxin/thioredoxin antioxidant system: A look at the pancreatic beta-cell oxidant defense. Vitam Horm *121*, 45-66. 10.1016/bs.vh.2022.11.001.
37. Rohli, K.E., Stubbe, N.J., Walker, E.M., Pearson, G.L., Soleimanpour, S.A., and Stephens, S.B. (2024). A metabolic redox relay supports ER proinsulin export in pancreatic islet beta cells. JCI Insight *9*. 10.1172/jci.insight.178725.
38. Hodson, D.J., Mitchell, R.K., Marselli, L., Pullen, T.J., Gimeno Brias, S., Semplici, F., Everett, K.L., Cooper, D.M., Bugliani, M., Marchetti, P., et al. (2014). ADCY5 couples

glucose to insulin secretion in human islets. Diabetes *63*, 3009-3021. 10.2337/db13-1607.
39. Guillemain, G., Khemtemourian, L., Brehat, J., Morin, D., Movassat, J., Tourrel-Cuzin, C., and Lacapere, J.J. (2024). TSPO in pancreatic beta cells and its possible involvement in type 2 diabetes. Biochimie *224*, 104-113. 10.1016/j.biochi.2024.06.007.
40. Gatliff, J., and Campanella, M. (2016). TSPO: kaleidoscopic 18-kDa amid biochemical pharmacology, control and targeting of mitochondria. Biochem J *473*, 107-121. 10.1042/BJ20150899.
41. Yadav, S.K., Kambis, T.N., Kar, S., Park, S.Y., and Mishra, P.K. (2020). MMP9 mediates acute hyperglycemia-induced human cardiac stem cell death by upregulating apoptosis and pyroptosis in vitro. Cell Death & Disease *11*, 186. 10.1038/s41419-020-2367-6.
42. Liu, C., Wan, X., Ye, T., Fang, F., Chen, X., Chen, Y., and Dong, Y. (2014). Matrix metalloproteinase 2 contributes to pancreatic Beta cell injury induced by oxidative stress. PLoS One *9*, e110227. 10.1371/journal.pone.0110227.
43. Rikka, S., Quinsay, M.N., Thomas, R.L., Kubli, D.A., Zhang, X., Murphy, A.N., and Gustafsson, Å.B. (2011). Bnip3 impairs mitochondrial bioenergetics and stimulates mitochondrial turnover. Cell Death & Differentiation *18*, 721-731. 10.1038/cdd.2010.146.
44. Aoyagi, K., Nishiwaki, C., Nakamichi, Y., Yamashita, S.-i., Kanki, T., and Ohara-Imaizumi, M. (2024). Imeglimin mitigates the accumulation of dysfunctional mitochondria to restore insulin secretion and suppress apoptosis of pancreatic β-cells from db/db mice. Scientific Reports *14*, 6178. 10.1038/s41598-024-56769-w.
45. Ellis, J.M., Li, L.O., Wu, P.C., Koves, T.R., Ilkayeva, O., Stevens, R.D., Watkins, S.M., Muoio, D.M., and Coleman, R.A. (2010). Adipose acyl-CoA synthetase-1 directs fatty acids toward beta-oxidation and is required for cold thermogenesis. Cell Metab *12*, 53-64. 10.1016/j.cmet.2010.05.012.
46. Teodoro, B.G., Sampaio, I.H., Bomfim, L.H., Queiroz, A.L., Silveira, L.R., Souza, A.O., Fernandes, A.M., Eberlin, M.N., Huang, T.Y., Zheng, D., et al. (2017). Long-chain acyl-CoA synthetase 6 regulates lipid synthesis and mitochondrial oxidative capacity in human and rat skeletal muscle. J Physiol *595*, 677-693. 10.1113/jp272962.
47. Bellini, L., Campana, M., Rouch, C., Chacinska, M., Bugliani, M., Meneyrol, K., Hainault, I., Lenoir, V., Denom, J., Véret, J., et al. (2018). Protective role of the ELOVL2/docosahexaenoic acid axis in glucolipotoxicity-induced apoptosis in rodent beta cells and human islets. Diabetologia *61*, 1780-1793. 10.1007/s00125-018-4629-8.
48. Gamble, K.L., Berry, R., Frank, S.J., and Young, M.E. (2014). Circadian clock control of endocrine factors. Nat Rev Endocrinol *10*, 466-475. 10.1038/nrendo.2014.78.
49. O'Neill, J.S., Maywood, E.S., Chesham, J.E., Takahashi, J.S., and Hastings, M.H. (2008). cAMP-Dependent Signaling as a Core Component of the Mammalian Circadian Pacemaker. Science *320*, 949-953. doi:10.1126/science.1152506.
50. Aguayo-Mazzucato, C., Koh, A., El Khattabi, I., Li, W.C., Toschi, E., Jermendy, A., Juhl, K., Mao, K., Weir, G.C., Sharma, A., and Bonner-Weir, S. (2011). Mafa expression

enhances glucose-responsive insulin secretion in neonatal rat beta cells. Diabetologia *54*, 583-593. 10.1007/s00125-010-2026-z.

51. Hang, Y., Yamamoto, T., Benninger, R.K., Brissova, M., Guo, M., Bush, W., Piston, D.W., Powers, A.C., Magnuson, M., Thurmond, D.C., and Stein, R. (2014). The MafA transcription factor becomes essential to islet β-cells soon after birth. Diabetes *63*, 1994-2005. 10.2337/db13-1001.
52. Schmitt, K., Grimm, A., Dallmann, R., Oettinghaus, B., Restelli, L.M., Witzig, M., Ishihara, N., Mihara, K., Ripperger, J.A., Albrecht, U., et al. (2018). Circadian Control of DRP1 Activity Regulates Mitochondrial Dynamics and Bioenergetics. Cell Metab *27*, 657-666 e655. 10.1016/j.cmet.2018.01.011.
53. Sidarala, V., Pearson, G.L., Parekh, V.S., Thompson, B., Christen, L., Gingerich, M.A., Zhu, J., Stromer, T., Ren, J., Reck, E.C., et al. (2020). Mitophagy protects β cells from inflammatory damage in diabetes. JCI Insight *5*. 10.1172/jci.insight.141138.
54. Levi-D'Ancona, E., Sidarala, V., and Soleimanpour, S.A. (2023). Complementary Approaches to Interrogate Mitophagy Flux in Pancreatic β-Cells. J Vis Exp. 10.3791/65789.
55. Leloup, C., Tourrel-Cuzin, C., Magnan, C., Karaca, M., Castel, J., Carneiro, L., Colombani, A.L., Ktorza, A., Casteilla, L., and Pénicaud, L. (2009). Mitochondrial reactive oxygen species are obligatory signals for glucose-induced insulin secretion. Diabetes *58*, 673-681. 10.2337/db07-1056.
56. Dobin, A., Davis, C.A., Schlesinger, F., Drenkow, J., Zaleski, C., Jha, S., Batut, P., Chaisson, M., and Gingeras, T.R. (2012). STAR: ultrafast universal RNA-seq aligner. Bioinformatics *29*, 15-21. 10.1093/bioinformatics/bts635.
57. Anders, S., Pyl, P.T., and Huber, W. (2014). HTSeq—a Python framework to work with high-throughput sequencing data. Bioinformatics *31*, 166-169. 10.1093/bioinformatics/btu638.
58. Anders, S., and Huber, W. (2010). Differential expression analysis for sequence count data. Genome Biology *11*, R106. 10.1186/gb-2010-11-10-r106.
59. Subramanian, A., Tamayo, P., Mootha, V.K., Mukherjee, S., Ebert, B.L., Gillette, M.A., Paulovich, A., Pomeroy, S.L., Golub, T.R., Lander, E.S., and Mesirov, J.P. (2005). Gene set enrichment analysis: A knowledge-based approach for interpreting genome-wide expression profiles. Proceedings of the National Academy of Sciences *102*, 15545-15550. doi:10.1073/pnas.0506580102.
60. Hughes, M.E., Hogenesch, J.B., and Kornacker, K. (2010). JTK_CYCLE: An Efficient Nonparametric Algorithm for Detecting Rhythmic Components in Genome-Scale Data Sets. Journal of Biological Rhythms *25*, 372-380. 10.1177/0748730410379711.
61. Brooks, T.G., Mrčela, A., Lahens, N.F., Paschos, G.K., Grosser, T., Skarke, C., FitzGerald, G.A., and Grant, G.R. (2022). Nitecap: An Exploratory Circadian Analysis Web Application. Journal of Biological Rhythms *37*, 43-52. 10.1177/07487304211054408.

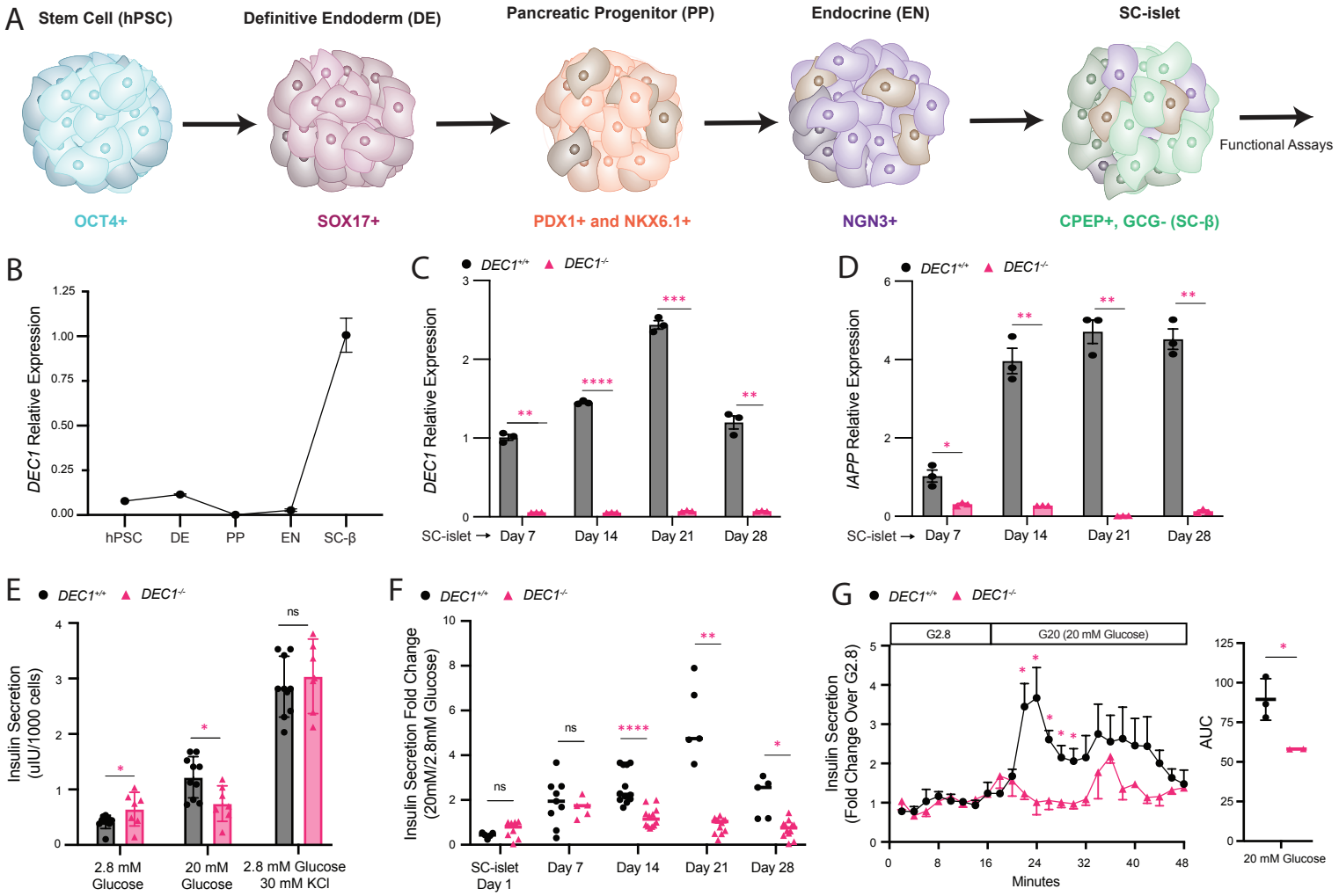
A
Stem Cell (hPSC)
Definitive Endoderm (DE)
Pancreatic Progenitor (PP)
Endocrine (EN)
SC-islet
Functional Assays
OCT4+
SOX17+
PDX1+ and NKX6.1+
NGN3+
CPEP+, GCG- (SC-β)
B
DEC1 Relative Expression
hPSC
DE
PP
EN
SC-β
C
DEC1+/+
DEC1-/-
DEC1 Relative Expression
SC-islet
Day 7
Day 14
Day 21
Day 28
D
IAPP Relative Expression
E
Insulin Secretion (uIU/1000 cells)
2.8 mM Glucose
20 mM Glucose
2.8 mM Glucose 30 mM KCl
ns
F
Insulin Secretion Fold Change (20mM/2.8mM Glucose)
SC-islet Day 1
G
G2.8
G20 (20 mM Glucose)
Insulin Secretion (Fold Change Over G2.8)
Minutes
AUC
20 mM Glucose

**Figure 1. DEC1 is required for mature insulin responses to glucose in human SC-islets.**

(A) Stepwise directed differentiation of SC-islets from human pluripotent stem cells (hPSC).
(B) *DEC1* expression is low through differentiation stages and selectively induced in SC-β cells. Data from N = 2 differentiations with n = 3 replicate measurements each, normalized to day 21 sorted SC-β cells.
(C-D) *DEC1* and *IAPP* expression are significantly reduced in *DEC1*$^{-/-}$ SC-islets from week 1 through week 4 of extended *in vitro* culture. Data from N = 1 differentiation with n = 3 replicate measurements, normalized to day 7 SC-islets.
(E) *DEC1*$^{-/-}$ SC-islets show immature glucose stimulated insulin secretion (GSIS) responses under the indicated sequential static incubations, marked by elevated insulin secretion under low (2.8 mM) glucose, and decreased insulin secretion under saturating (20 mM) glucose. Data from week 2 *DEC1*$^{+/+}$ (N=5 differentiations, n = 50-100 SC-islets each) and *DEC1*$^{-/-}$ (N=4 differentiations, n = 50-100 SC-islets each) lines.
(F) *DEC1*$^{-/-}$ SC-islets fail to expand GSIS responses during extended *in vitro* culture. Data are insulin secretion fold-change between sequential static 2.8mM and 20mM glucose incubations of *DEC1*$^{+/+}$ (N=5 differentiations, n = 50-100 SC-islets each) and *DEC1*$^{-/-}$ (N=4 differentiations, n = 50-100 SC-islets each) SC-islets at day 1, 7, 14, 21, and 28.
(G) GSIS dynamics reveal *DEC1*$^{-/-}$ SC-islets have low peak (first phase) insulin secretion under saturating (20 mM) glucose and dampened second phase secretion, consistent with an immature phenotype. Data from week 2 *DEC1*$^{+/+}$ (N=1 differentiation, n = 50-100 islets) and *DEC1*$^{-/-}$ SC-islets (N=1 differentiation, n = 50-100 islets) perifused with the indicated substrates, normalized to the mean of the first incubation. Area under the curve (AUC) are summarized to the right.

Data are mean ± SEM. *p <0.05, **p <1e-2, ***p <1e-3, ****p <1e-4, unpaired t test [(E), (F), and (G)] and Wilcoxon test [(C) and (D)].

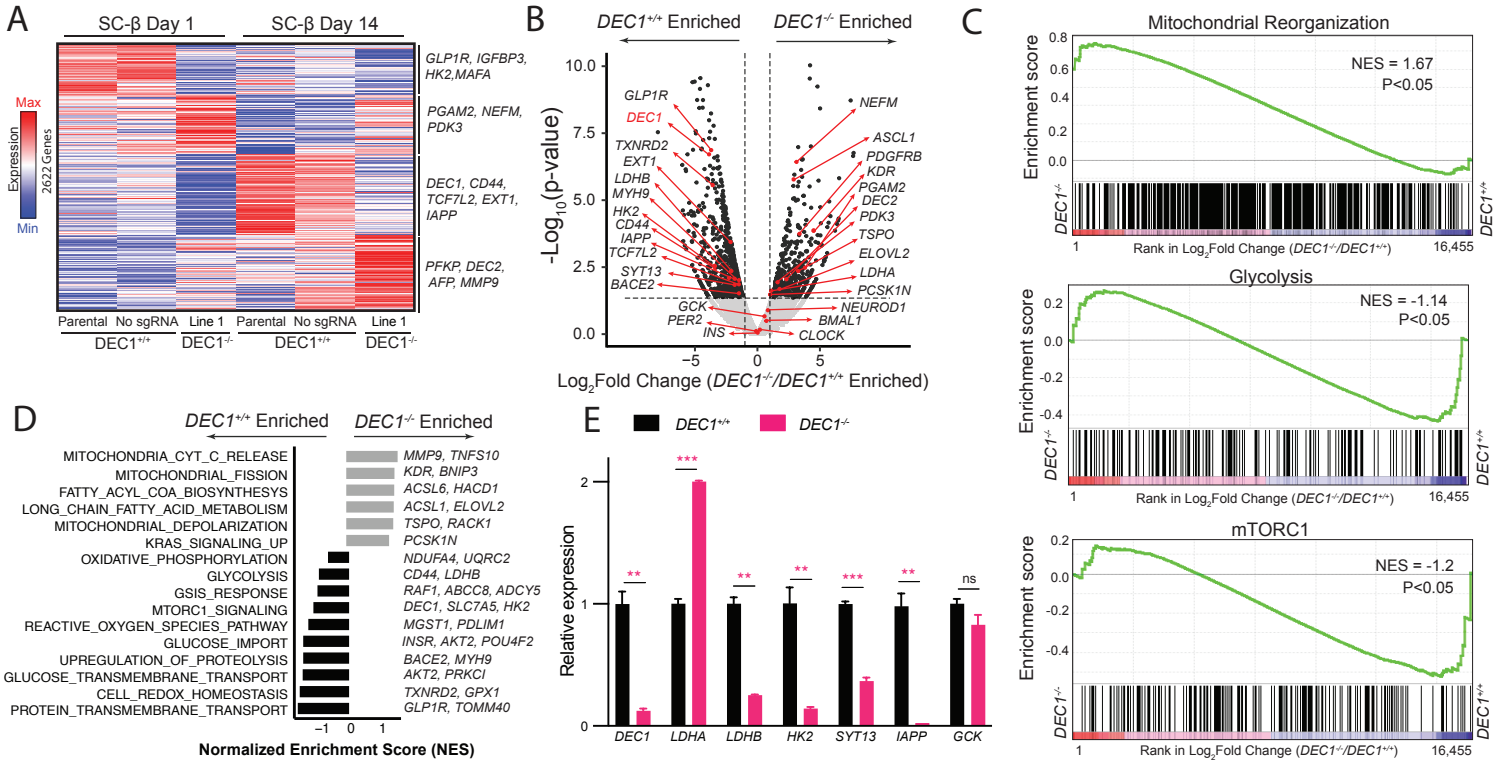
A
SC-β Day 1
SC-β Day 14
Max
Expression
2622 Genes
Min
GLP1R, IGFBP3, HK2,MAFA
PGAM2, NEFM, PDK3
DEC1, CD44, TCF7L2, EXT1, IAPP
PFKP, DEC2, AFP, MMP9
Parental
No sgRNA
Line 1
DEC1+/+
DEC1-/-
B
DEC1+/+ Enriched
DEC1-/- Enriched
-Log10(p-value)
Log2Fold Change (DEC1-/-/DEC1+/+ Enriched)
GLP1R
DEC1
TXNRD2
EXT1
LDHB
MYH9
HK2
CD44
IAPP
TCF7L2
SYT13
BACE2
GCK
PER2
INS
NEFM
ASCL1
PDGFRB
KDR
PGAM2
DEC2
PDK3
TSPO
ELOVL2
LDHA
PCSK1N
NEUROD1
BMAL1
CLOCK
C
Mitochondrial Reorganization
NES = 1.67
P<0.05
Glycolysis
NES = -1.14
P<0.05
mTORC1
NES = -1.2
P<0.05
Enrichment score
Rank in Log2Fold Change (DEC1-/-/DEC1+/+)
16,455
D
DEC1+/+ Enriched
DEC1-/- Enriched
MITOCHONDRIA_CYT_C_RELEASE
MITOCHONDRIAL_FISSION
FATTY_ACYL_COA_BIOSYNTHESYS
LONG_CHAIN_FATTY_ACID_METABOLISM
MITOCHONDRIAL_DEPOLARIZATION
KRAS_SIGNALING_UP
OXIDATIVE_PHOSPHORYLATION
GLYCOLYSIS
GSIS_RESPONSE
MTORC1_SIGNALING
REACTIVE_OXYGEN_SPECIES_PATHWAY
GLUCOSE_IMPORT
UPREGULATION_OF_PROTEOLYSIS
GLUCOSE_TRANSMEMBRANE_TRANSPORT
CELL_REDOX_HOMEOSTASIS
PROTEIN_TRANSMEMBRANE_TRANSPORT
MMP9, TNFS10
KDR, BNIP3
ACSL6, HACD1
ACSL1, ELOVL2
TSPO, RACK1
PCSK1N
NDUFA4, UQRC2
CD44, LDHB
RAF1, ABCC8, ADCY5
DEC1, SLC7A5, HK2
MGST1, PDLIM1
INSR, AKT2, POU4F2
BACE2, MYH9
AKT2, PRKCI
TXNRD2, GPX1
GLP1R, TOMM40
Normalized Enrichment Score (NES)
E
DEC1+/+
DEC1-/-
Relative expression
DEC1
LDHA
LDHB
HK2
SYT13
IAPP
GCK
ns
F
DEC1+/+ Enriched
DEC1-/- Enriched
β-Cell Genes
Log2Fold change (DEC1-/-/DEC1+/+)
GLP1R
CD44
PAX4
G6PC2
TCF7L2
PDX1
SYT13
IAPP
GIPR
ISL1
RFX6
BMP5
VDR
DPP4
NEFM
Glucose Metabolism
TPBG
ISG20
HK2
EXT1
SOX9
LDHB
TGFA
QSOX1
SDC1
FUT8
CHST2
NDUFA4
TCIRG1
PKP2
EGFR
GPC4
AGRN
Glucose Import and Sensing
SLC2A14
POU4F2
SLC1A2
PLA2G1B
KLF15
OSTN
TERT
RNASEL
SORBS1
PKC and cAMP
ADCY5
ADCY3
ADCY6
PRKCQ
PRKCD
Disallowed Genes
LDHA
PDK3
PDGFRA
PDGFRB
ALB
PGAM2
AFP

**Figure 2. DEC1 regulates β-cell maturity-linked effectors of glucose metabolism and insulin secretion**

(A) *DEC1* ablation in SC-β cells results in 2,622 differentially expressed genes. Heatmap shows differentially expressed genes, row-normalized z-score, ($p < 0.05$, DEseq test) in CD49a-sorted SC-β cells in Parental, No sgRNA, and *DEC1*$^{-/-}$ Line 1 at day 1 and day 14 of *in vitro* maturation.

(B) *DEC1*$^{-/-}$ depleted genes include SC-β maturity-linked genes (*GLP1R*, *IAPP*, and *SYT13*). Volcano plot shows all differentially expressed genes. Genes with ≥2-fold change and p-value < 0.05 are in black. Genes of particular interest are highlighted.

(C) Mitochondrial reorganization genes are enriched in *DEC1*$^{-/-}$ SC-β, whereas glycolysis and mTORC1 genes are enriched in *DEC1*$^{+/+}$ SC-β cells. Gene set enrichment analysis shows genes ranked by fold change in *DEC1*$^{-/-}$ vs. *DEC1*$^{+/+}$ SC-β cells. NES, normalized enrichment score.

(D) *DEC1* ablation disrupts suppression of lipid metabolism genes and induction of glucose stimulated insulin secretion (GSIS), glucose import, and redox homeostasis genes in SC-β cells. Gene set enrichment analysis shows pathways enriched in *DEC1*$^{-/-}$ vs. *DEC1*$^{+/+}$ SC-β cells.

(E) Relative expression of selected genes from (B). Data are qPCR from day 21 SC-β cells. N = 1 differentiation, n = 3 technical replicates each. Data are mean ± SEM. *p <0.01, **p <1e-2, ***p <1e-3, Wilcoxon test.

(F) *DEC1* ablation leads to upregulation of genes disallowed in mature β cells (*LDHA*, *PDK3*, *ALB* and *AFP*) while downregulating key glucose metabolism genes (*LDHB* and *NDUFA4*) and insulin secretion genes (*TCF7L2*, *SYT13*, *ADCY5* and *ADCY3*). Shown are fold changes of genes in the indicated enriched β cell-related gene sets.

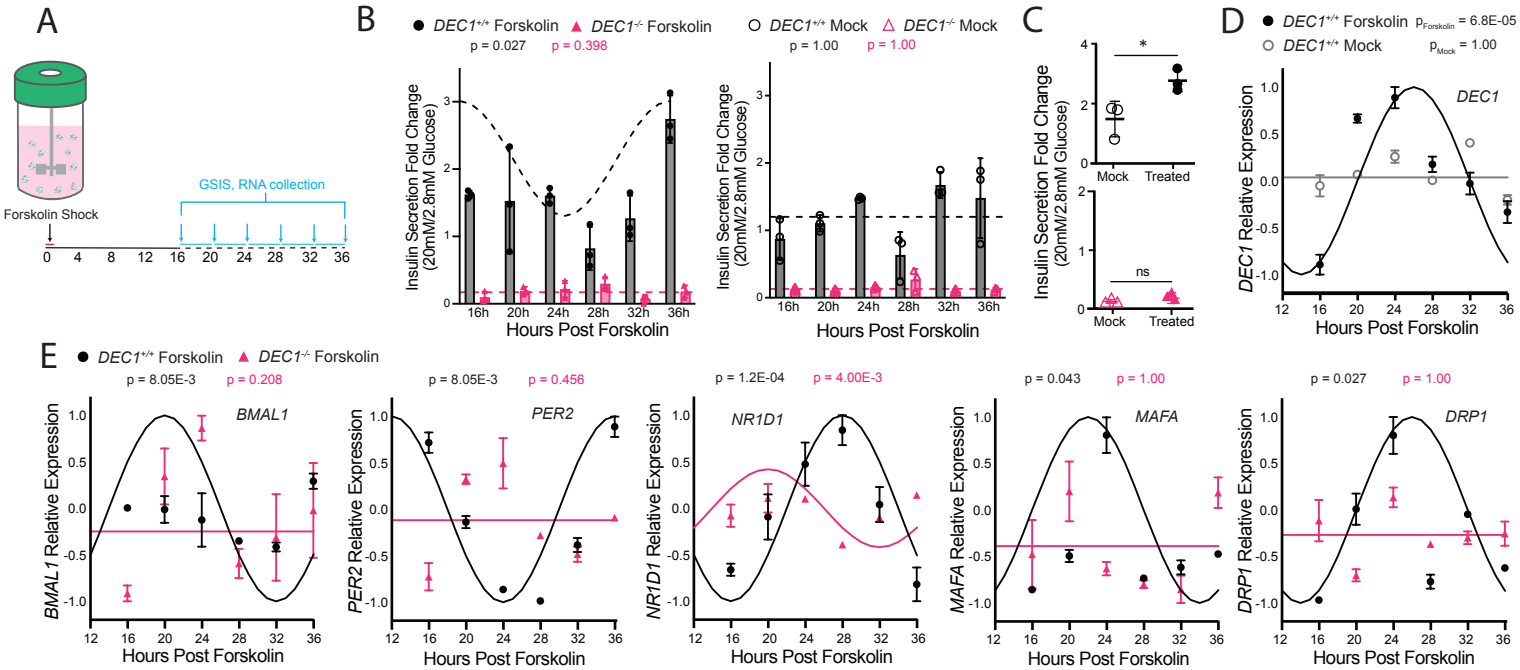
A
Forskolin Shock
GSIS, RNA collection
0 4 8 12 16 20 24 28 32 36
B
DEC1+/+ Forskolin
DEC1-/- Forskolin
p = 0.027
p = 0.398
DEC1+/+ Mock
DEC1-/- Mock
p = 1.00
p = 1.00
Insulin Secretion Fold Change (20mM/2.8mM Glucose)
16h 20h 24h 28h 32h 36h
Hours Post Forskolin
C
*
ns
Mock
Treated
D
DEC1+/+ Forskolin
p_Forskolin = 6.8E-05
DEC1+/+ Mock
p_Mock = 1.00
DEC1
DEC1 Relative Expression
Hours Post Forskolin
E
DEC1+/+ Forskolin
DEC1-/- Forskolin
p = 8.05E-3
p = 0.208
BMAL1
BMAL1 Relative Expression
p = 8.05E-3
p = 0.456
PER2
PER2 Relative Expression
p = 1.2E-04
p = 4.00E-3
NR1D1
NR1D1 Relative Expression
p = 0.043
p = 1.00
MAFA
MAFA Relative Expression
p = 0.027
p = 1.00
DRP1
DRP1 Relative Expression
Hours Post Forskolin

**Figure 3. DEC1 controls circadian insulin secretion and gene expression rhythms in human SC-islets**.

(A) Experimental design for synchronization with 10μM forskolin. Glucose stimulated insulin secretion (GSIS) and RNA were assayed at 4 hour intervals 16 hours after forskolin shock.

(B) *DEC1* is required for circadian SC-islet insulin secretion responses. Insulin secretion fold change follows a circadian rhythm (rhythmicity p-value < 0.05) in *DEC1*$^{+/+}$ SC-islets vs *DEC1*$^{-/-}$ SC-islets following forskolin shock, with mock-treated controls shown to the right (N = 1 differentiation, n = 50-100 SC-islets). Shown are detrended (baseline-subtracted) mean ± SEM insulin secretion fold changes at 16h post forskolin shock and every 4h after. Rhythmicity p-value by JTK analysis.

(C) Insulin secretion fold-change is 2-fold greater in synchronized *DEC1*$^{+/+}$ SC-islets at the circadian peak time (36h post forskolin shock) compared to mock controls. Data are mean ± SEM. *p <0.05, unpaired t-test.

(D) Circadian *DEC1* expression following forskolin synchronization in *DEC1*$^{+/+}$ SC-islets. Data is relative expression (N = 1 differentiation with n = 3 replicate measurements).

(E) *DEC1* loss prevents circadian synchronization of key clock regulators (*BMAL1* and *PER2*) and SC-β cell genes (*MAFA* and *DRP1*). Data from N = 1 differentiation with n = 3 replicate measurements.

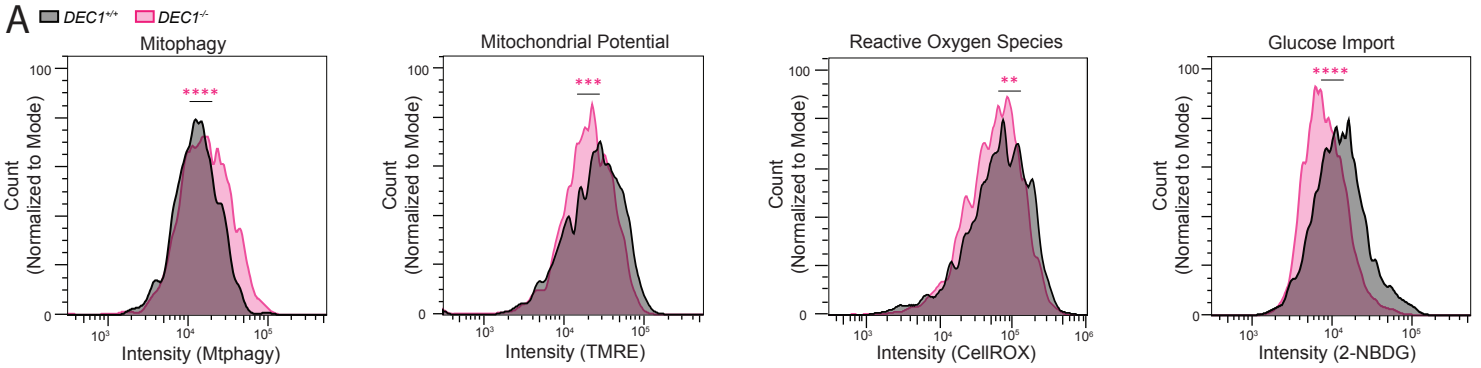
A
DEC1+/+
DEC1-/-
Mitophagy
Mitochondrial Potential
Reactive Oxygen Species
Glucose Import
Count (Normalized to Mode)
Intensity (Mtphagy)
Intensity (TMRE)
Intensity (CellROX)
Intensity (2-NBDG)

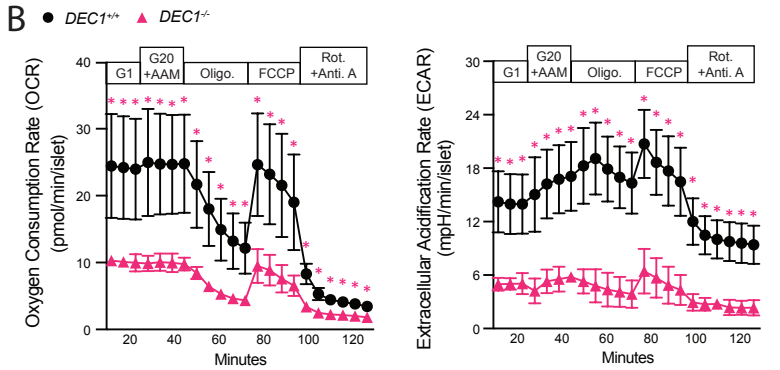
B
DEC1+/+
DEC1-/-
G1
G20 +AAM
Oligo.
FCCP
Rot. +Anti. A
Oxygen Consumption Rate (OCR) (pmol/min/islet)
Extracellular Acidification Rate (ECAR) (mpH/min/islet)
Minutes

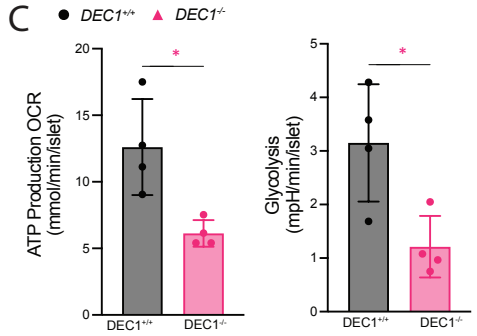
C
DEC1+/+
DEC1-/-
ATP Production OCR (mmol/min/islet)
Glycolysis (mpH/min/islet)

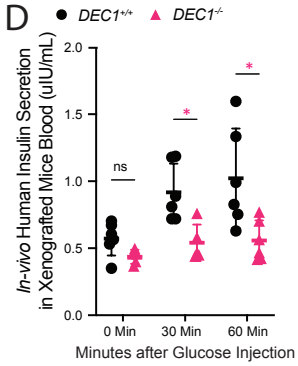
D
DEC1+/+
DEC1-/-
In-vivo Human Insulin Secretion in Xenografted Mice Blood (uIU/mL)
ns
0 Min
30 Min
60 Min
Minutes after Glucose Injection

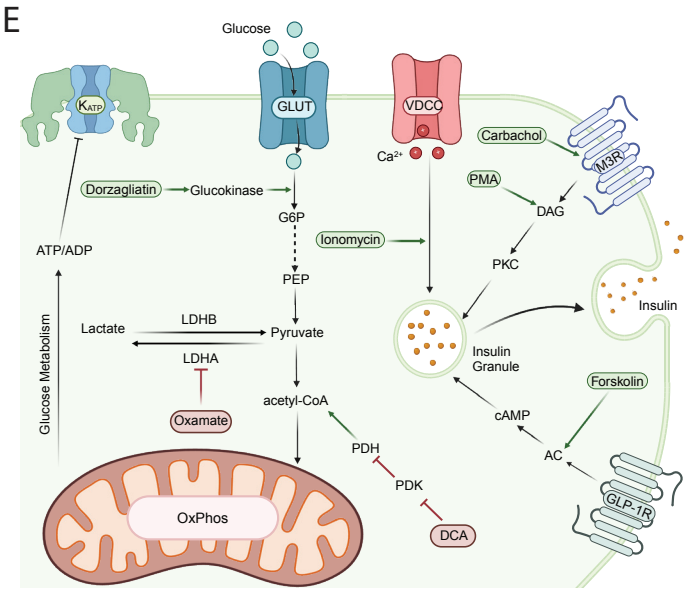
E
Glucose
GLUT
KATP
VDCC
Ca2+
Carbachol
M3R
PMA
DAG
Dorzagliatin
Glucokinase
G6P
Ionomycin
PKC
ATP/ADP
PEP
Insulin
Lactate
LDHB
Pyruvate
LDHA
Insulin Granule
Glucose Metabolism
Forskolin
Oxamate
acetyl-CoA
cAMP
PDH
AC
PDK
GLP-1R
OxPhos
DCA

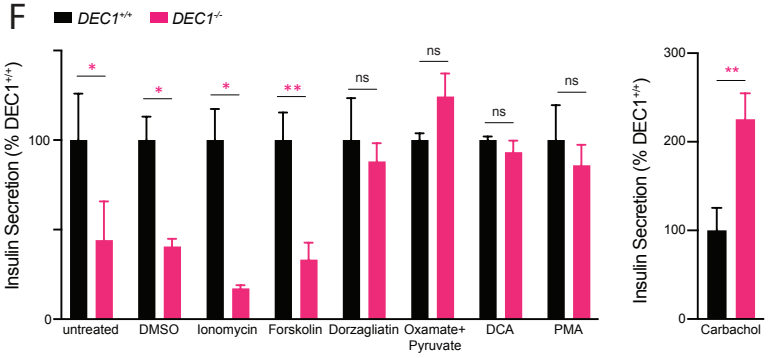
F
DEC1+/+
DEC1-/-
Insulin Secretion (% DEC1+/+)
untreated
DMSO
Ionomycin
Forskolin
Dorzagliatin
Oxamate+ Pyruvate
DCA
PMA
Carbachol

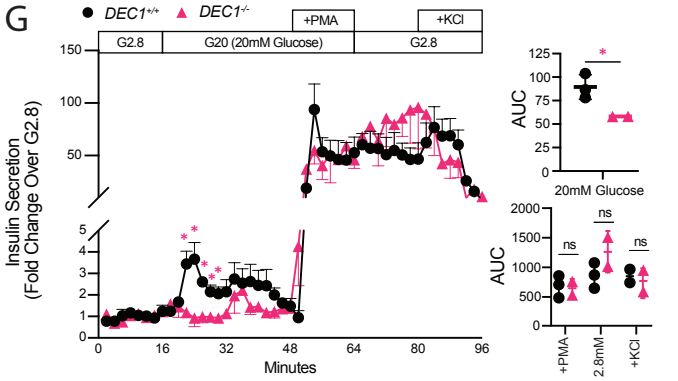
G
DEC1+/+
DEC1-/-
G2.8
G20 (20mM Glucose)
+PMA
+KCl
Insulin Secretion (Fold Change Over G2.8)
Minutes
AUC
20mM Glucose
+PMA
2.8mM
+KCl
ns

**Figure 4. DEC1 sustains mitochondrial integrity and bioenergetics in maturing SC-β cells.**

**(A)** *DEC1*-ablated SC-β cells exhibit mitochondria with increased autophagy and reduced membrane potential, along with lower reactive oxygen species generation and glucose import. Data are distributions, normalized to mode, of flow cytometry for mitophagy (Mtphagy staining), mitochondrial membrane potential (TMRE staining), cellular reactive oxygen species (CellROX staining) and glucose uptake (2-NBDG staining) in CD49a-gated SC-β cells (N = 1 differentiation, n ≥ 1000 cells).

**(B)** *DEC1* loss stifles oxygen consumption rates (OCR, left) and extracellular acidification rates (ECAR, right). Data from day 14 *DEC1*$^{+/+}$ and *DEC1*$^{-/-}$ SC-islets in response to 20mM glucose and a physiological amino acid mixture (G20+AAM); oligomycin; FCCP; and rotenone with antimycin A. Data are mean ± SEM from N = 1 differentiation with n =4 replicate measurements of 8 similar-sized SC-islets.

**(C)** ATP production-linked respiration (left) and glycolysis (left) rates are impaired in *DEC1*$^{-/-}$ SC-islets. Data from N = 1 differentiation with n = 4 replicate measurements of 8 similar-sized SC-islets.

**(D)** Glucose stimulated insulin secretion defect in *DEC1*-knockout SC-islets is not rescued by *in vivo* transplant. Data are serum human insulin secreted into blood of fasted immunodeficient mice transplanted with *DEC1*$^{+/+}$ or *DEC1*$^{-/-}$ SC-islets before, 30 minutes, and 60 minutes after intraperitoneal glucose injection 21 weeks post-transplantation. Data are mean ± SEM from N = 4-6 mice with n = 2 replicate measurements each.

**(E)** Pathway of glucose metabolism and downstream signaling targeted by insulinotropic agents screened for GSIS rescue experiments.

**(F-G)** Glucose-independent PKC activator PMA, muscarinic receptor agonist carbachol, and metabolic flux enhancers (oxamate with methyl-pyruvate, DCA, and dorzagliatin) restore insulin secretion in *DEC1*$^{-/-}$ SC-islets under sequential static glucose incubations (F) (2.8 to 20mM glucose) or dynamic conditions for PMA (G) relative to *DEC1*$^{+/+}$ SC-islets. Data from N = 1 differentiation with n = 2-3 replicate measurements of 50-100 SC-islets.

Data are mean ± SEM. *p <0.05, **p <1e-2, ***p <1e-3, ****p <1e-4, Wilcoxon test (A), and unpaired t tests [(B), (C), (D), (F) and (G)].

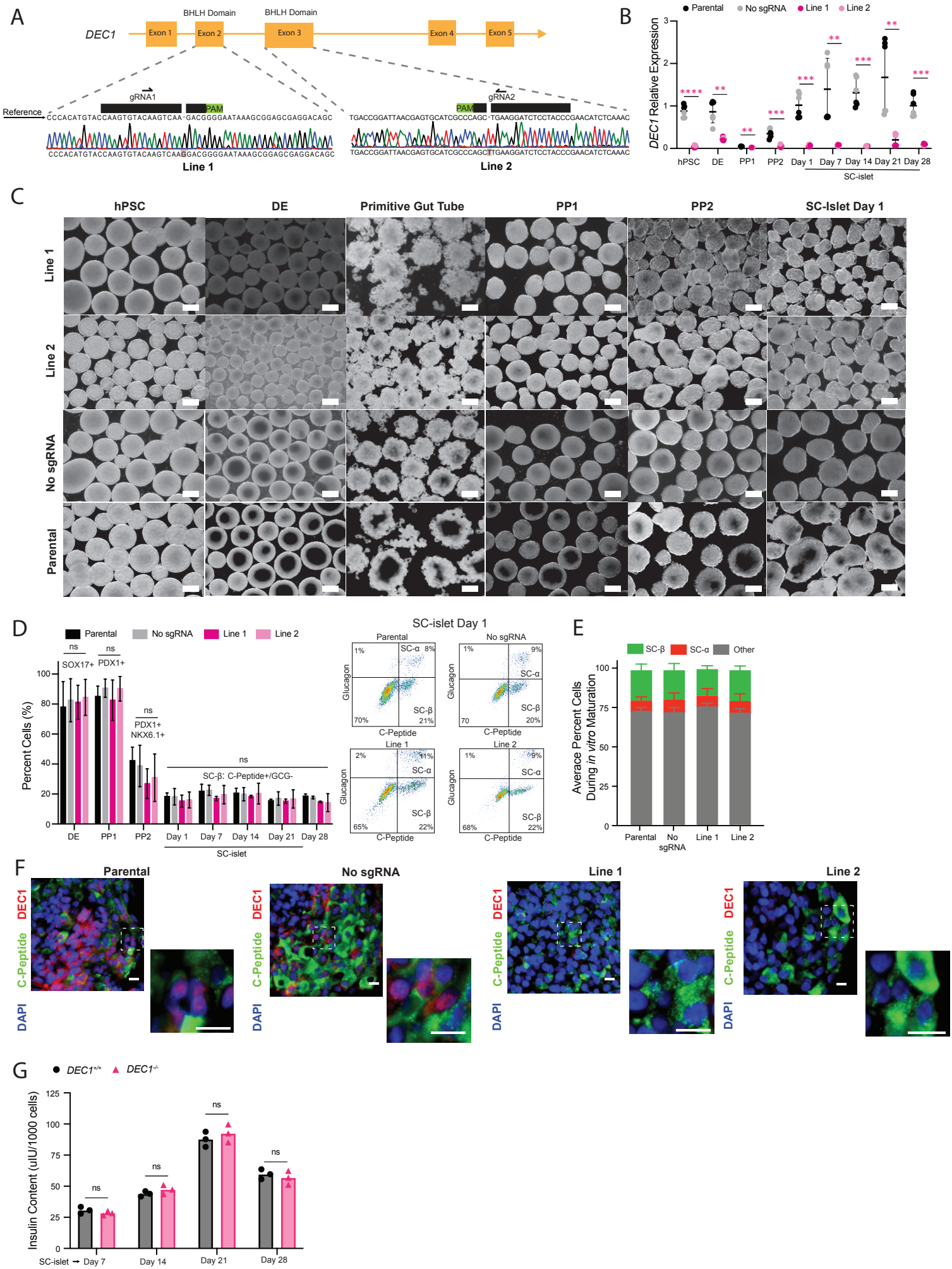
A
DEC1
BHLH Domain
BHLH Domain
Exon 1
Exon 2
Exon 3
Exon 4
Exon 5
gRNA1
gRNA2
PAM
Reference
CCCACATGTACCAAGTGTACAAGTCAA-GACGGGGAATAAAGCGGAGCGAGGACAGC
TGACCGGATTAACGAGTGCATCGCCCAGC-TGAAGGATCTCCTACCCGAACATCTCAAAC
Line 1
Line 2
B
Parental
No sgRNA
Line 1
Line 2
DEC1 Relative Expression
hPSC
DE
PP1
PP2
Day 1
Day 7
Day 14
Day 21
Day 28
SC-islet
C
hPSC
DE
Primitive Gut Tube
PP1
PP2
SC-Islet Day 1
Line 1
Line 2
No sgRNA
Parental
D
Parental
No sgRNA
Line 1
Line 2
SOX17+
PDX1+
PDX1+ NKX6.1+
SC-β: C-Peptide+/GCG-
Percent Cells (%)
SC-islet
SC-islet Day 1
Glucagon
C-Peptide
SC-α
SC-β
E
SC-β
SC-α
Other
Averace Percent Cells During in vitro Maturation
Parental
No sgRNA
Line 1
Line 2
F
Parental
No sgRNA
Line 1
Line 2
DEC1
C-Peptide
DAPI
G
DEC1+/+
DEC1-/-
Insulin Content (uIU/1000 cells)
SC-islet → Day 7
Day 14
Day 21
Day 28

**Supplementary Figure 1. DEC1 has no effect on SC-islet differentiation, composition, or insulin production. Related to Figure 1.**

(A) Strategy to generate *DEC1*$^{-/-}$ hPSC lines for subsequent differentiation. Shown are CRISPR/Cas9 sgRNAs used to create two *DEC1*$^{-/-}$ hPSC lines, along with sequencing results indicating homozygous knockout due to frameshift-causing base-pair insertions.
(B) *DEC1* expression is abrogated throughout *in vitro* differentiation and maturation of SC-islets generated from *DEC1*$^{-/-}$ hPSC lines. Data from N = 1 Differentiations with n = 3 replicate measurements.
(C) 3D SC-islet organoids form normally from *DEC1*$^{-/-}$ hPSC lines. Data are brightfield images of 3D organoids throughout differentiation. Scale bar is 100um.
(D) SC-islets differentiate normally from *DEC1*-ablated hPSC lines. Data quantify the indicated cell populations by flow cytometry for the indicated differentiation markers (N = 5 differentiations, n ≥ 2000 cells each). Representative flow cytometry data are shown to the right.
(E) SC-islet composition is not affected by DEC1 loss. Data is average of SC-β (C-Peptide+/Glucagon-), and SC-α (Glucagon+) cells across day 7, 14, 21 and 28 for the indicated lines (N = 5 differentiations, n ≥ 2000 cells each).
(F) C-Peptide and DEC1 immunostaining of week 2 *DEC1*$^{+/+}$ and *DEC1*$^{-/-}$ SC-islets. Scale bar is 10um.
(G) *DEC1*-ablated SC-islets produce insulin normally. Data is insulin content from day 7, 14, 21 and 28 *DEC1*$^{+/+}$ and *DEC1*$^{-/-}$ SC-islets (N=1 differentiation, n = 30-80 SC-islets each).

Data are mean ± SEM. *p <0.05, **p <1e-2, ***p <1e-3, ****p <1e-4, Wilcoxon test (B), multiple unpaired t tests (against Parental) [(D) and (E)], and unpaired t test (G).

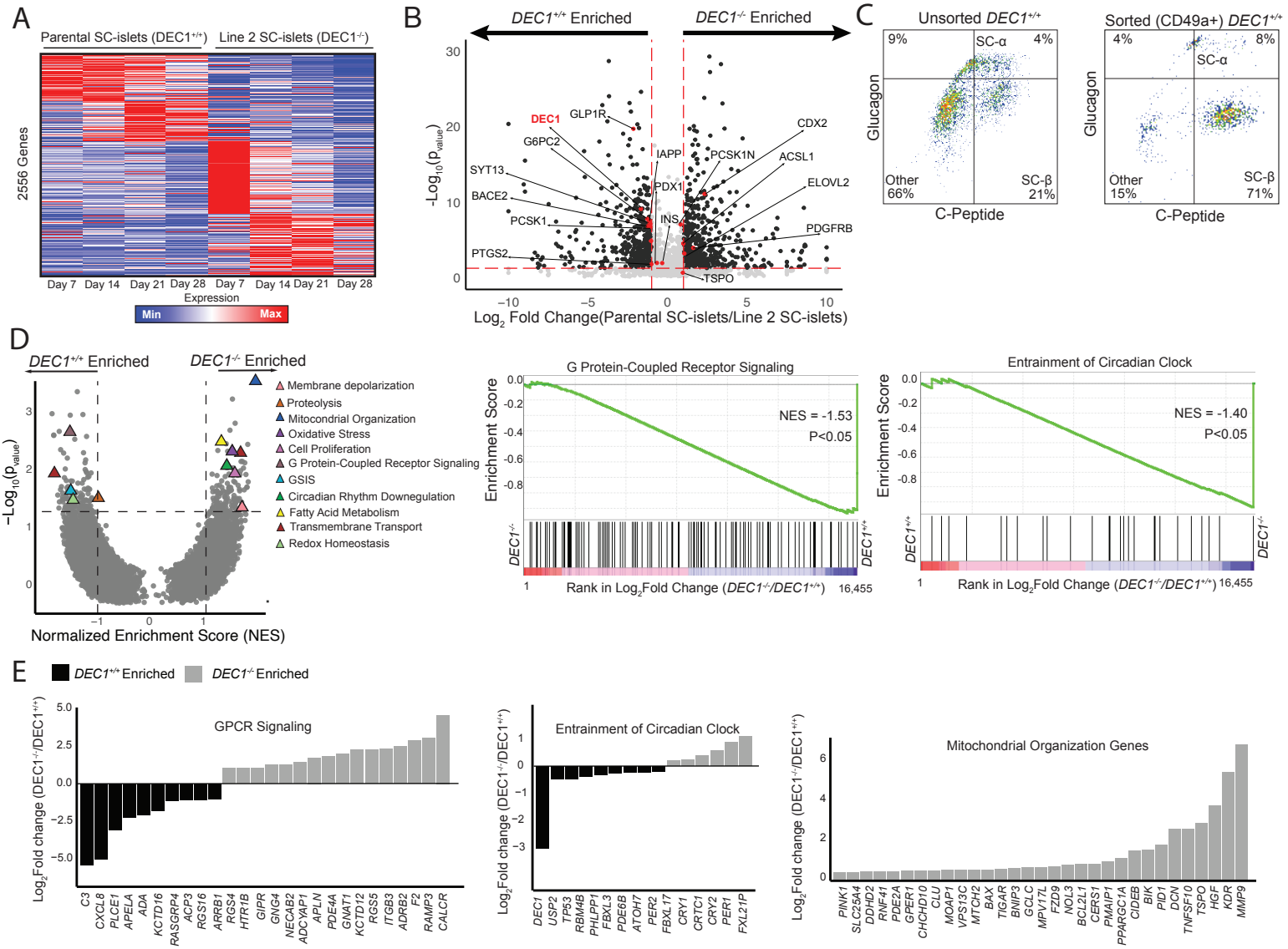
A
Parental SC-islets (DEC1+/+)
Line 2 SC-islets (DEC1-/-)
2556 Genes
Day 7 Day 14 Day 21 Day 28 Day 7 Day 14 Day 21 Day 28
Expression
Min
Max
B
DEC1+/+ Enriched
DEC1-/- Enriched
-Log10(pvalue)
DEC1
GLP1R
G6PC2
SYT13
BACE2
PCSK1
PTGS2
IAPP
PDX1
INS
PCSK1N
CDX2
ACSL1
ELOVL2
PDGFRB
TSPO
Log2 Fold Change(Parental SC-islets/Line 2 SC-islets)
C
Unsorted DEC1+/+
Sorted (CD49a+) DEC1+/+
Glucagon
C-Peptide
9%
SC-α
4%
Other 66%
SC-β 21%
4%
SC-α
8%
Other 15%
SC-β 71%
D
DEC1+/+ Enriched
DEC1-/- Enriched
-Log10(pvalue)
Normalized Enrichment Score (NES)
Membrane depolarization
Proteolysis
Mitocondrial Organization
Oxidative Stress
Cell Proliferation
G Protein-Coupled Receptor Signaling
GSIS
Circadian Rhythm Downegulation
Fatty Acid Metabolism
Transmembrane Transport
Redox Homeostasis
G Protein-Coupled Receptor Signaling
Enrichment Score
NES = -1.53
P<0.05
DEC1-/-
DEC1+/+
Rank in Log2Fold Change (DEC1-/-/DEC1+/+)
16,455
Entrainment of Circadian Clock
NES = -1.40
P<0.05
E
DEC1+/+ Enriched
DEC1-/- Enriched
GPCR Signaling
Log2Fold change (DEC1-/-/DEC1+/+)
C3 CXCL8 PLCE1 APELA ADA KCTD16 RASGRP4 ACP3 RGS16 ARRB1 RGS4 HTR1B GIPR GNG4 NECAB2 ADCYAP1 APLN PDE4A GNAT1 KCTD12 RGS5 ITGB3 ADRB2 F2 RAMP3 CALCR
Entrainment of Circadian Clock
DEC1 USP2 TP53 RBM4B PHLPP1 FBXL3 PDE6B ATOH7 PER2 FBXL17 CRY1 CRTC1 CRY2 PER1 FXL21P
Mitochondrial Organization Genes
PINK1 SLC25A4 DDHD2 RNF41 PDE2A GPER1 CHCHD10 CLU MOAP1 VPS13C MTCH2 BAX TIGAR BNIP3 GCLC MPV17L FZD9 NOL3 BCL2L1 CERS1 PMAIP1 PPARGC1A CIDEB BIK PID1 DCN TNFSF10 TSPO HGF KDR MMP9

**Supplementary Figure 2. Additional gene set enrichment analysis of *DEC1*$^{-/-}$ SC-β cells. Related to Figure 2.**

(A) *DEC1* ablation in SC-islet organoids results in 2,556 differentially expressed genes. Heatmap shows differentially expressed genes ($p < 0.05$, DEseq test) in Parental and *DEC1*$^{-/-}$ Line 2 SC-islets at days 7, 14, 21, and 28 of *in vitro* maturation.

(B) *DEC1*$^{-/-}$ depleted genes include many SC-β maturity-linked genes (*GLP1R*, *IAPP*, *SYT13*, *PCSK1*, and *G6PC2*). Volcano plot shows all differentially expressed genes at day 21 of SC-islet *in-vitro* maturation. Genes with at least a 2-fold change and p-value less than 0.05 are in black. Genes of particular interest are highlighted.

(C) CD49a live-cell-sorting enables RNA sequencing of highly enriched SC-β population. n = 2000 cells.

(D) *DEC1* ablation in SC-β cells results in dysregulation of important β-cell processes (p-value > 0.05 and absolute NES value > 1) (left). Gene set enrichment analysis shows genes ranked by fold change in *DEC1*$^{-/-}$ vs. *DEC1*$^{+/+}$ SC-β cells (middle and right). NES, normalized enrichment score.

(E) *DEC1* ablation in SC-β cells upregulates mitochondrial autophagy related (*PINK1*, *BNIP3*) and mitochondrial membrane depolarization (*BIK*, *TSPO*, *MMP9*) genes. Shown are fold changes of genes in the indicated enriched β cell-related gene sets.

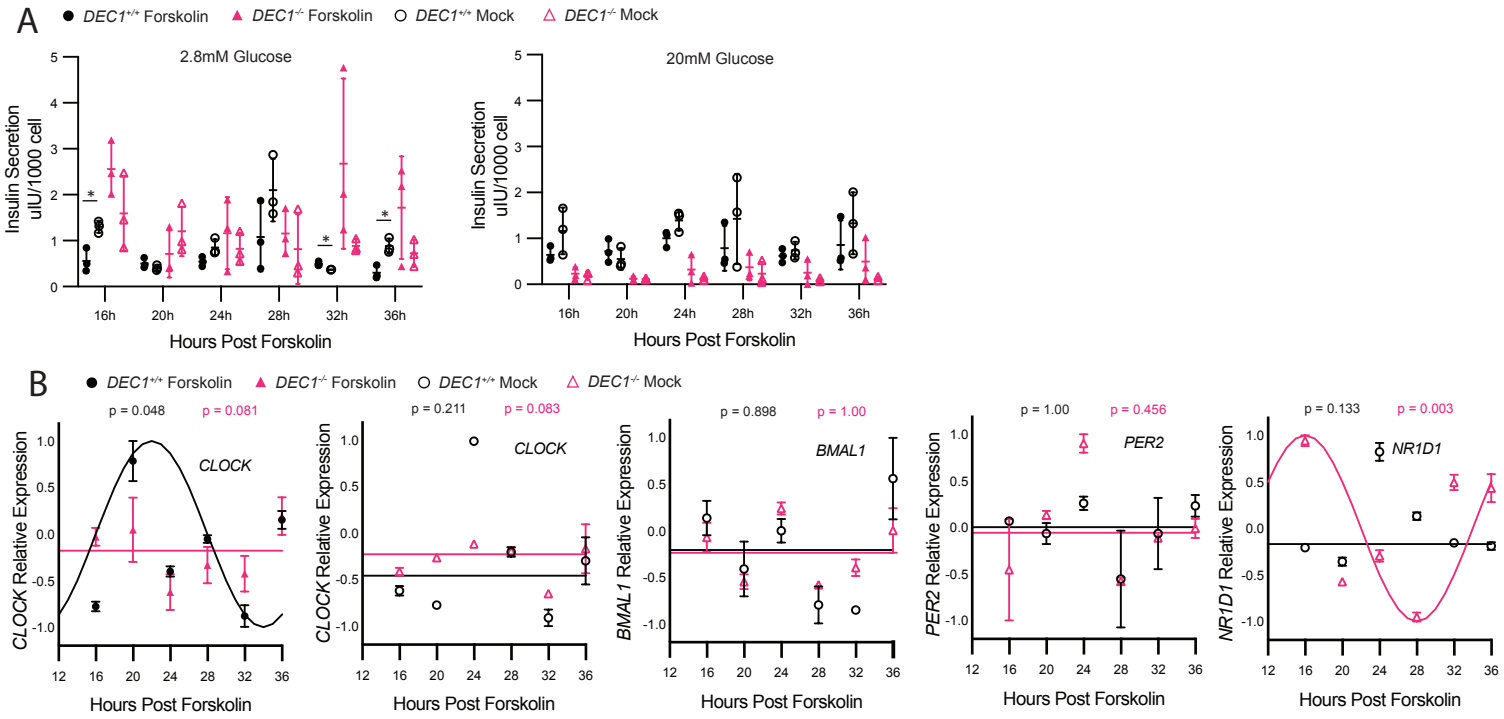
A
DEC1+/+ Forskolin
DEC1-/- Forskolin
DEC1+/+ Mock
DEC1-/- Mock
2.8mM Glucose
20mM Glucose
Insulin Secretion uIU/1000 cell
Hours Post Forskolin
16h
20h
24h
28h
32h
36h
B
p = 0.048
p = 0.081
CLOCK
p = 0.211
p = 0.083
CLOCK
p = 0.898
p = 1.00
BMAL1
p = 1.00
p = 0.456
PER2
p = 0.133
p = 0.003
NR1D1
CLOCK Relative Expression
BMAL1 Relative Expression
PER2 Relative Expression
NR1D1 Relative Expression
Hours Post Forskolin

**Supplementary Figure 3. Circadian insulin secretion and clock gene expression in *DEC1*$^{+/+}$ and *DEC1*$^{-/-}$ SC-islets. Related to Figure 3.**

(A) Circadian GSIS response with reduced basal (2.8mM glucose) insulin secretion at 16 and 36 hours post forskolin treatment in *DEC1*$^{+/+}$ SC-islets (left). Insulin secretion during 20mM glucose is shown to the right. Data are mean ± SEM. *p <0.05, unpaired t-test.

(B) *DEC1* loss disrupts circadian synchronization of the indicated genes. Data are relative expression under forskolin or mock treatments (N = 1 differentiation with n =3 replicate measurements). Shown are detrended (baseline-subtracted) mean ± SEM insulin secretion fold changes at 16h post forskolin shock and every 4h after. Rhythmicity p-value by JTK analysis.

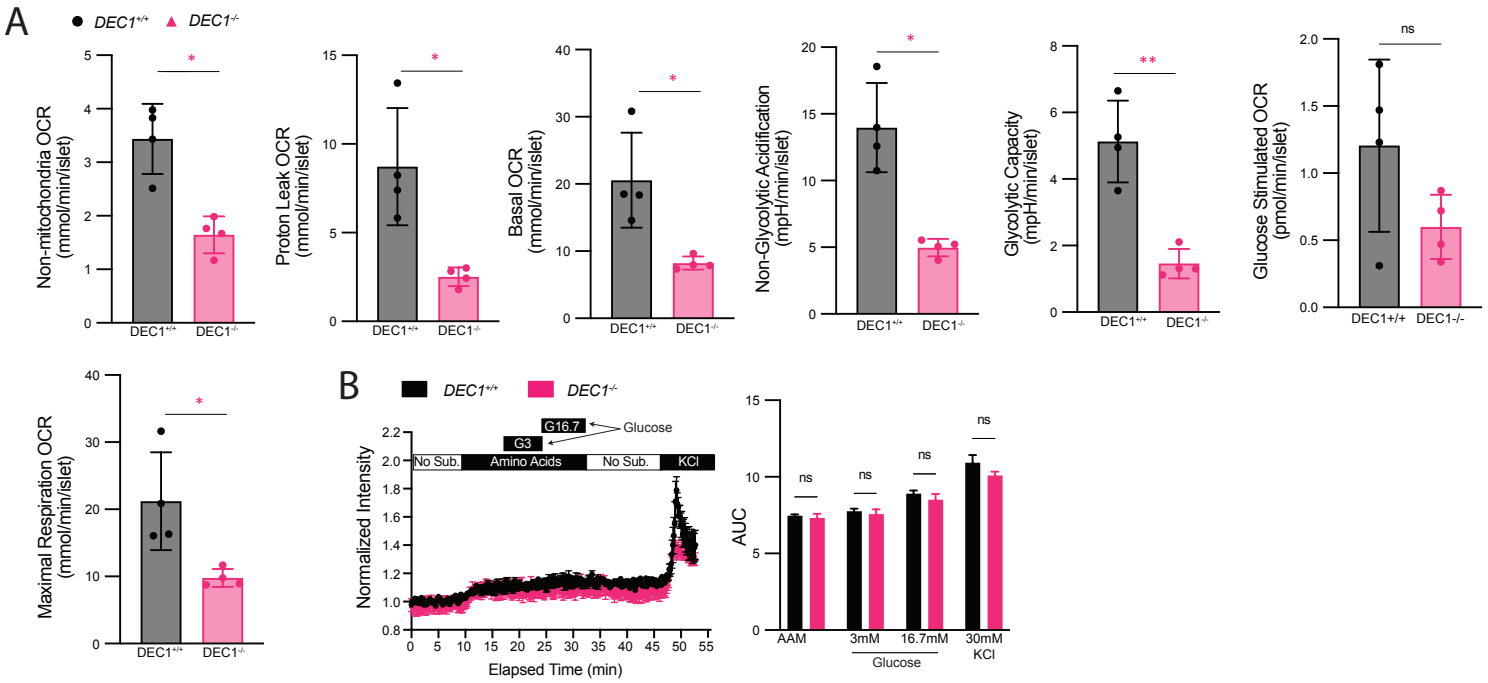
A
DEC1+/+
DEC1-/-
Non-mitochondria OCR (mmol/min/islet)
Proton Leak OCR (mmol/min/islet)
Basal OCR (mmol/min/islet)
Non-Glycolytic Acidification (mpH/min/islet)
Glycolytic Capacity (mpH/min/islet)
Glucose Stimulated OCR (pmol/min/islet)
DEC1+/+
DEC1-/-
ns
Maximal Respiration OCR (mmol/min/islet)
B
Normalized Intensity
Elapsed Time (min)
No Sub.
Amino Acids
No Sub.
KCl
G16.7
G3
Glucose
AUC
AAM
3mM
16.7mM
30mM KCl
Glucose

**Supplementary Figure 4**. **DEC1 regulates glycolytic and oxidative metabolism in maturing SC-β cells. Related to Figure 4.**

**(A)** Decreases in the indicated features determined by oxygen consumption rate (OCR) and extracellular acidification rate (ECAR) analysis of *DEC1*$^{-/-}$ SC-islets. Data from Figure 4B experiments (N = 1 differentiation with n = 4 replicate measurements of 8 similar-sized SC-islets).

**(B)** $Ca^{2+}$ influx measured by Fura-2 staining in response to no substrate (No Sub.); a physiological mixture of amino acids (AAM); AAM supplemented with 3mM glucose (G3); AAM supplemented with 16.7mM glucose (G16.7); no glucose; and 30 mM KCl, with respective AUCs quantified to the right. N=1 differentiation, n = 3 replicates with 8-12 similar-sized SC-islets. Data are mean ± SEM. *p <0.05, **p <1e-2, unpaired t-test.